

We are committed to providing [accessible customer service](#).

If you need accessible formats or communications supports, please [contact us](#).

Nous tenons à améliorer [l'accessibilité des services à la clientèle](#).

Si vous avez besoin de formats accessibles ou d'aide à la communication, veuillez [nous contacter](#).

**2022 Work Report**  
**RLX PROPERTY**  
**Helicopter Borne SkyTEM**  
**Magnetic and Electromagnetic Survey**  
**Red Lake Area, Ontario**  
**Solstice Gold Corp.**

**Work Conducted:** November 5 to November 15, 2021

**NTS:** 052N05, 052N06, 052N12

**Date Submitted:** June 13, 2022

**Work Conducted and Reported by:**

**SkyTEM Surveys ApS, Denmark**

**Assessment Report prepared by:**

Bruce A. Barham, MSc., PGO

Senior Geologist

**For:** Solstice Gold Corp.

## Table of Contents

Table of Contents .....	2
List of Figures .....	2
List of Tables.....	2
1.0 SUMMARY .....	3
2.0 INTRODUCTION – EXPLORATION TARGET .....	3
3.0 PROPERTY DESCRIPTION, LOCATION .....	6
4.0 ACCESS, PHYSIOGRPAHY, CLIMATE, LOCAL RESOURCES .....	8
5.0 HISTORY.....	10
6.0 REGIONAL AND LOCAL GEOLOGY .....	13
6.1 Regional Geology .....	13
6.2 Local Rock Types and Structural Geology .....	15
6.3 Mineralization .....	16
7.0 EXPLORATION.....	17
8.0 INTERPRETATION .....	18
9.0 RECOMMENDATIONS.....	21
10.0 REFERENCES.....	22
APPENDIX A: Statement of Qualifications.....	24
APPENDIX B: Report.....	26

## List of Figures

Figure 1: RLX Property Location.....	5
Figure 2: RLX Claims .....	9
Figure 3: Red Lake Area, Regional Geology, Property Access.....	11
Figure 4: Bowdidge (2005) Geology 4B: Total Field Magnetic Results (2022: This Report) .....	14

## List of Tables

Table 1: SkyTEM Airborne Survey Basic Statistics.....	4
Table 2: RLX Property Claims .....	6
Table 3: Dome Exploration Diamond Drilling.....	12
Table 4: SkyTEM Survey Details .....	18
Table 5: Recommended Future Work.....	21

## **1.0 SUMMARY**

This report presents the results of a helicopter-borne magnetic and electromagnetic survey completed by the contractor SkyTEM Surveys ApS over an eleven-day period from November 5 to 15 2021 for Solstice Gold Corp (Solstice) over its RLX Property northwest of Red Lake, Ontario. The survey was conducted as part of Solstice's overall exploration program to identify and further delineate subsurface targets for drilling on the Property. The SkyTEM312M system collected time domain electromagnetic and magnetic data whose final products include processed data, grids, and maps in Geosoft format, inversion results, and modelled layer conductivity. These geophysical products show the electromagnetic characteristics of the subsurface that will guide an interpretation of the geological structure of the Property and delineate targets for further detailed exploration. The results of the survey confirm the presence of the electromagnetic anomalies reported by the Ontario Geological Survey (2008) and define layer parallel anomalies predominantly within a north – south magnetic low. An inversion model of the electromagnetic results also suggests conductive response is stronger at depth. Previous exploration results completed in the area of the property are also described in this report.

Additional exploration beginning with geological mapping and prospecting is recommended. Barham (2022) reports on a previously completed (February 2021) magnetic-only survey also covering a significant portion of the existing RLX Property. The coordinate system used throughout the report is NAD 1983 UTM Zone 15N.

## **2.0 INTRODUCTION – EXPLORATION TARGET**

Solstice is a gold explorer with expertise in the Red Lake area. Its RLX Property, in the Nungesser Lake area northwest of Red Lake, is poorly exposed and has only seen limited exploration in the past. The RLX Property is transected by structures that can be traced directly to gold deposits near Red Lake. Assessment records record rock types on the RLX Property important in the stratigraphy of some Red Lake gold mines. Solstice has initiated the exploration of the RLX Property for its lode gold potential.

This report introduces the results of a helicopter-borne airborne magnetic and electromagnetic survey conducted over the RLX Property, Red Lake area, Ontario, in November 2021 for Solstice Gold Corp. A previous helicopter-borne magnetic-only survey completed in February 2021 is reported in Barham (2022). This high-resolution magnetic and electromagnetic survey was flown by SkyTEM Surveys ApS (Denmark) between November 5 and November 15, 2021. A full survey description including daily logs, flight parameters, instrumentation, data acquisition, post survey processing, and representative maps are given in Appendix B. Some of this is summarized below in Table 1.



**Table 1: SkyTEM Airborne Survey Basic Statistics**

Full Survey Statistics (see report Appendix B)		
Contractor: SkyTEM Surveys ApS    Survey Flown Nov 5-15 2021		
Survey Size	879.1	Line Km
Direction	Az 90/270	Line Azimuths – NS Tie-lines

The SkyTEM312M system collects time domain electromagnetic and magnetic data along with supporting navigation measurements.

Appendix A provides project costs and other details pertinent to this submission. A technical report, prepared by SkyTEM provides the details of the survey in Appendix B. Figure 1 shows the location of the RLX property.

This report is prepared by B. Barham who assisted in the design of the survey, collated the acquired data and prepared the maps for this report.

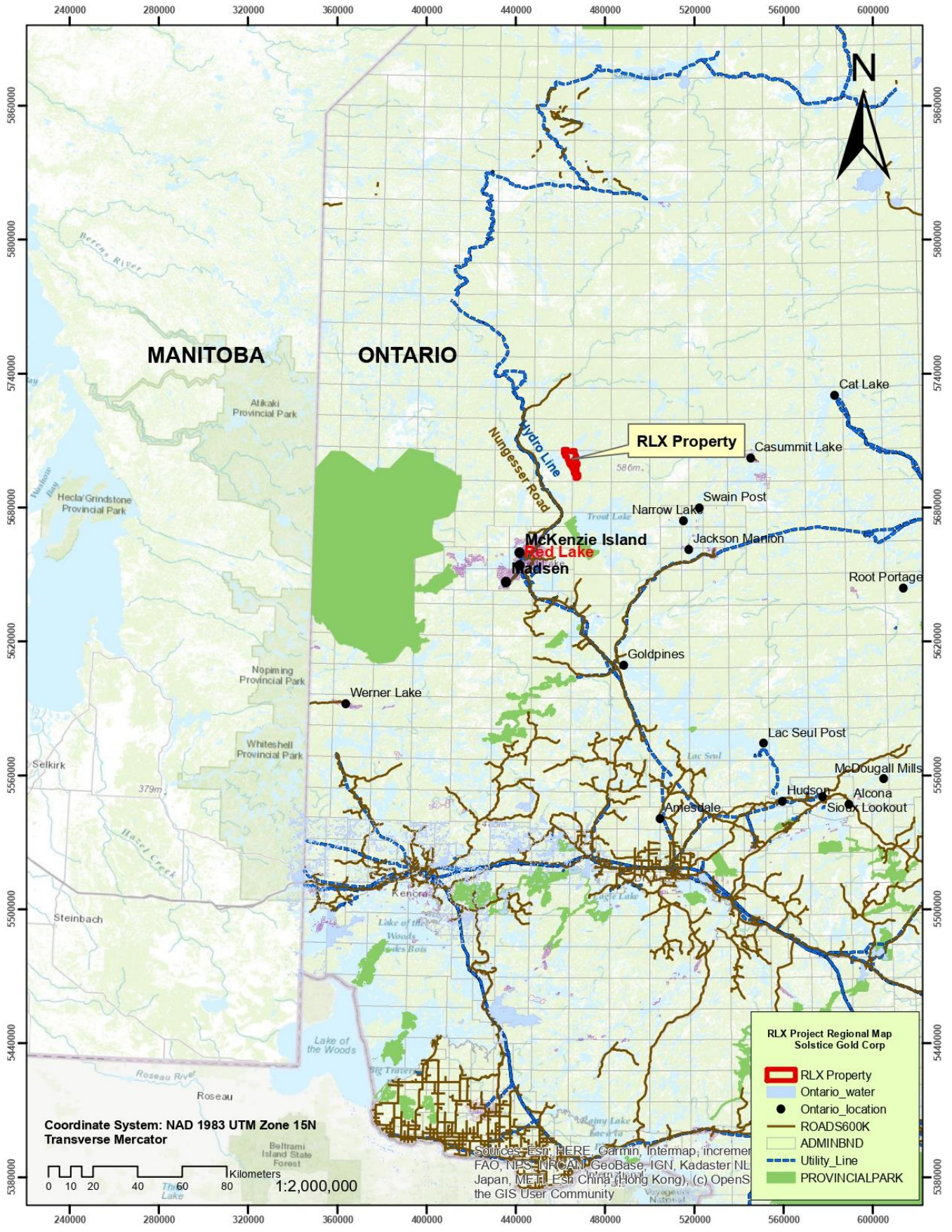


Figure 1: RLX Property Location

### 3.0 PROPERTY DESCRIPTION, LOCATION

The RLX Property is located about 40 kilometers north-northeast of the Balmertown townsite and consists of multicell claims as shown on Figure 2 and listed in Table 2. The RLX Property is comprised of 121 claims, including 111 Single-Cell Mining Claim and 10 Multi-cell Mining Claims located in management areas of Hanton Lake, Nungesser Lake, Storey Lake and Sobelski Lake within Red Lake Mining Division.

The RLX Property presented in the report is comprised of 121 claims, including 111 Single-Cell Mining Claims and 10 Multi-cell Mining Claims located in the townships of Hanton Lake, Nungesser Lake, Pringle Lake, Storey Lake and Sobeski Lake within the Red Lake Mining Division.

All claims included into the assessment report are active and 100% (10004221) Solstice Gold Corp. recorded in MLAS Ontario. 10 Multi-cell Mining Claims denoted by “\*” were registered By Gravel Ridge Resources Ltd. (10002746) on 2021-01-26. The claims were subject to different option agreements between Gravel Ridge Resources Ltd., and Solstice Gold Corporation whereby Solstice becomes 100% owner and claims were transferred 100% to Solstice Gold Corporation on 2022-01-04. 111 Cell claims denoted by “\*\*” were registered by Martin Tunney (10003651) (a principal of Solstice Gold) on 2021-02-19 and transferred 100% to (10004221) Solstice Gold Corp on 2021-03-16.

**Table 2: RLX Property Claims**

Number	Township	Tenure	Issued	Anniversary	Required	Applied	Reserve	Holder	Note
632352	HANTON LAKE ,NUNGESSER LAKE	MC	2021-01-26	2024-01-26	9600	9600	89	Solstice Gold Corp. (10004221)	*
632353	HANTON LAKE ,NUNGESSER LAKE	MC	2021-01-26	2024-01-26	6800	6800	0	Solstice Gold Corp. (10004221)	*
632354	NUNGESSER LAKE ,PRINGLE LAKE	MC	2021-01-26	2024-01-26	10000	10000	92	Solstice Gold Corp. (10004221)	*
632355	HANTON LAKE ,NUNGESSER LAKE ,PRINGLE LAKE ,STOREY LAKE	MC	2021-01-26	2024-01-26	9600	9600	0	Solstice Gold Corp. (10004221)	*
632356	NUNGESSER LAKE	MC	2021-01-26	2024-01-26	6400	6400	0	Solstice Gold Corp. (10004221)	*
632357	HANTON LAKE ,NUNGESSER LAKE	MC	2021-01-26	2024-01-26	7200	7200	0	Solstice Gold Corp. (10004221)	*
632360	HANTON LAKE	MC	2021-01-26	2024-01-26	2400	2400	0	Solstice Gold Corp. (10004221)	*
632361	HANTON LAKE	MC	2021-01-26	2024-01-26	2800	2800	0	Solstice Gold Corp. (10004221)	*
632362	HANTON LAKE	MC	2021-01-26	2024-01-26	5200	5200	0	Solstice Gold Corp. (10004221)	*
632363	HANTON LAKE	MC	2021-01-26	2024-01-26	5600	5600	0	Solstice Gold Corp. (10004221)	*
638413	SOBESKI LAKE	SC	2021-02-19	2023-02-19	400	0	0	Solstice Gold Corp. (10004221)	**
638414	SOBESKI LAKE	SC	2021-02-19	2023-02-19	400	0	0	Solstice Gold Corp. (10004221)	**
638415	SOBESKI LAKE	SC	2021-02-19	2023-02-19	400	0	0	Solstice Gold Corp. (10004221)	**
638416	SOBESKI LAKE	SC	2021-02-19	2023-02-19	400	0	0	Solstice Gold Corp. (10004221)	**
638417	SOBESKI LAKE	SC	2021-02-19	2023-02-19	400	0	0	Solstice Gold Corp. (10004221)	**
638418	SOBESKI LAKE	SC	2021-02-19	2023-02-19	400	0	0	Solstice Gold Corp. (10004221)	**
638419	SOBESKI LAKE	SC	2021-02-19	2023-02-19	400	0	0	Solstice Gold Corp. (10004221)	**
638420	HANTON LAKE ,SOBESKI LAKE	SC	2021-02-19	2023-02-19	400	0	0	Solstice Gold Corp. (10004221)	**
638421	HANTON LAKE ,SOBESKI LAKE	SC	2021-02-19	2023-02-19	400	0	0	Solstice Gold Corp. (10004221)	**
638422	HANTON LAKE ,SOBESKI LAKE	SC	2021-02-19	2023-02-19	400	0	0	Solstice Gold Corp. (10004221)	**
638423	HANTON LAKE ,SOBESKI LAKE	SC	2021-02-19	2023-02-19	400	0	0	Solstice Gold Corp. (10004221)	**
638424	HANTON LAKE ,SOBESKI LAKE	SC	2021-02-19	2023-02-19	400	0	0	Solstice Gold Corp. (10004221)	**
638425	HANTON LAKE ,SOBESKI LAKE	SC	2021-02-19	2023-02-19	400	0	0	Solstice Gold Corp. (10004221)	**
638426	HANTON LAKE	SC	2021-02-19	2023-02-19	400	0	0	Solstice Gold Corp. (10004221)	**
638427	HANTON LAKE	SC	2021-02-19	2023-02-19	400	0	0	Solstice Gold Corp. (10004221)	**



Number	Township	Tenure	Issued	Anniversary	Required	Applied	Reserve	Holder	Note
638485	HANTON LAKE	SC	2021-02-19	2023-02-19	400	0	0	Solstice Gold Corp. (10004221)	**
638486	HANTON LAKE	SC	2021-02-19	2023-02-19	400	0	0	Solstice Gold Corp. (10004221)	**
638487	HANTON LAKE	SC	2021-02-19	2023-02-19	400	0	0	Solstice Gold Corp. (10004221)	**
638488	HANTON LAKE	SC	2021-02-19	2023-02-19	400	0	0	Solstice Gold Corp. (10004221)	**
638489	HANTON LAKE	SC	2021-02-19	2023-02-19	400	0	0	Solstice Gold Corp. (10004221)	**
638490	HANTON LAKE	SC	2021-02-19	2023-02-19	400	0	0	Solstice Gold Corp. (10004221)	**
638491	HANTON LAKE	SC	2021-02-19	2023-02-19	400	0	0	Solstice Gold Corp. (10004221)	**
638492	HANTON LAKE	SC	2021-02-19	2023-02-19	400	0	0	Solstice Gold Corp. (10004221)	**
638493	HANTON LAKE	SC	2021-02-19	2023-02-19	400	0	0	Solstice Gold Corp. (10004221)	**
638494	HANTON LAKE	SC	2021-02-19	2023-02-19	400	0	0	Solstice Gold Corp. (10004221)	**
638495	HANTON LAKE	SC	2021-02-19	2023-02-19	400	0	0	Solstice Gold Corp. (10004221)	**
638496	HANTON LAKE	SC	2021-02-19	2023-02-19	400	0	0	Solstice Gold Corp. (10004221)	**
638497	HANTON LAKE	SC	2021-02-19	2023-02-19	400	0	0	Solstice Gold Corp. (10004221)	**
638498	HANTON LAKE	SC	2021-02-19	2023-02-19	400	0	0	Solstice Gold Corp. (10004221)	**
638499	HANTON LAKE	SC	2021-02-19	2023-02-19	400	0	0	Solstice Gold Corp. (10004221)	**
638500	HANTON LAKE	SC	2021-02-19	2023-02-19	400	0	0	Solstice Gold Corp. (10004221)	**
638501	HANTON LAKE	SC	2021-02-19	2023-02-19	400	0	0	Solstice Gold Corp. (10004221)	**
638502	HANTON LAKE	SC	2021-02-19	2023-02-19	400	0	0	Solstice Gold Corp. (10004221)	**
638503	HANTON LAKE	SC	2021-02-19	2023-02-19	400	0	0	Solstice Gold Corp. (10004221)	**
638504	HANTON LAKE	SC	2021-02-19	2023-02-19	400	0	0	Solstice Gold Corp. (10004221)	**
638505	HANTON LAKE	SC	2021-02-19	2023-02-19	400	0	0	Solstice Gold Corp. (10004221)	**
638506	HANTON LAKE	SC	2021-02-19	2023-02-19	400	0	0	Solstice Gold Corp. (10004221)	**
638507	HANTON LAKE	SC	2021-02-19	2023-02-19	400	0	0	Solstice Gold Corp. (10004221)	**
638508	HANTON LAKE	SC	2021-02-19	2023-02-19	400	0	0	Solstice Gold Corp. (10004221)	**
638509	HANTON LAKE	SC	2021-02-19	2023-02-19	400	0	0	Solstice Gold Corp. (10004221)	**
638510	HANTON LAKE	SC	2021-02-19	2023-02-19	400	0	0	Solstice Gold Corp. (10004221)	**
638511	HANTON LAKE	SC	2021-02-19	2023-02-19	400	0	0	Solstice Gold Corp. (10004221)	**
638512	HANTON LAKE	SC	2021-02-19	2023-02-19	400	0	0	Solstice Gold Corp. (10004221)	**
638513	HANTON LAKE	SC	2021-02-19	2023-02-19	400	0	0	Solstice Gold Corp. (10004221)	**
638514	HANTON LAKE	SC	2021-02-19	2023-02-19	400	0	0	Solstice Gold Corp. (10004221)	**
638515	HANTON LAKE	SC	2021-02-19	2023-02-19	400	0	0	Solstice Gold Corp. (10004221)	**
638516	HANTON LAKE	SC	2021-02-19	2023-02-19	400	0	0	Solstice Gold Corp. (10004221)	**
638517	HANTON LAKE	SC	2021-02-19	2023-02-19	400	0	0	Solstice Gold Corp. (10004221)	**
638518	HANTON LAKE	SC	2021-02-19	2023-02-19	400	0	0	Solstice Gold Corp. (10004221)	**
638519	HANTON LAKE	SC	2021-02-19	2023-02-19	400	0	0	Solstice Gold Corp. (10004221)	**
638520	HANTON LAKE	SC	2021-02-19	2023-02-19	400	0	0	Solstice Gold Corp. (10004221)	**
638521	HANTON LAKE	SC	2021-02-19	2023-02-19	400	0	0	Solstice Gold Corp. (10004221)	**
638522	HANTON LAKE	SC	2021-02-19	2023-02-19	400	0	0	Solstice Gold Corp. (10004221)	**
638523	HANTON LAKE	SC	2021-02-19	2023-02-19	400	0	0	Solstice Gold Corp. (10004221)	**

#### 4.0 ACCESS, PHYSIOGRPAHY, CLIMATE, LOCAL RESOURCES

Red Lake, Ontario is a full-service community where lodging, groceries, field gear, vehicle rentals and shipping can be arranged. Additionally, fishing lodges are sometimes available to provide lodging and logistical support for exploration.

The physiography of the project area is characterized by flat to gently undulating terrain with local topographic highs ranging to 50 meters above stream valleys. The Property is mixed mature and logged boreal forest consisting of black spruce in lowlands alternating with pine dominated areas on higher



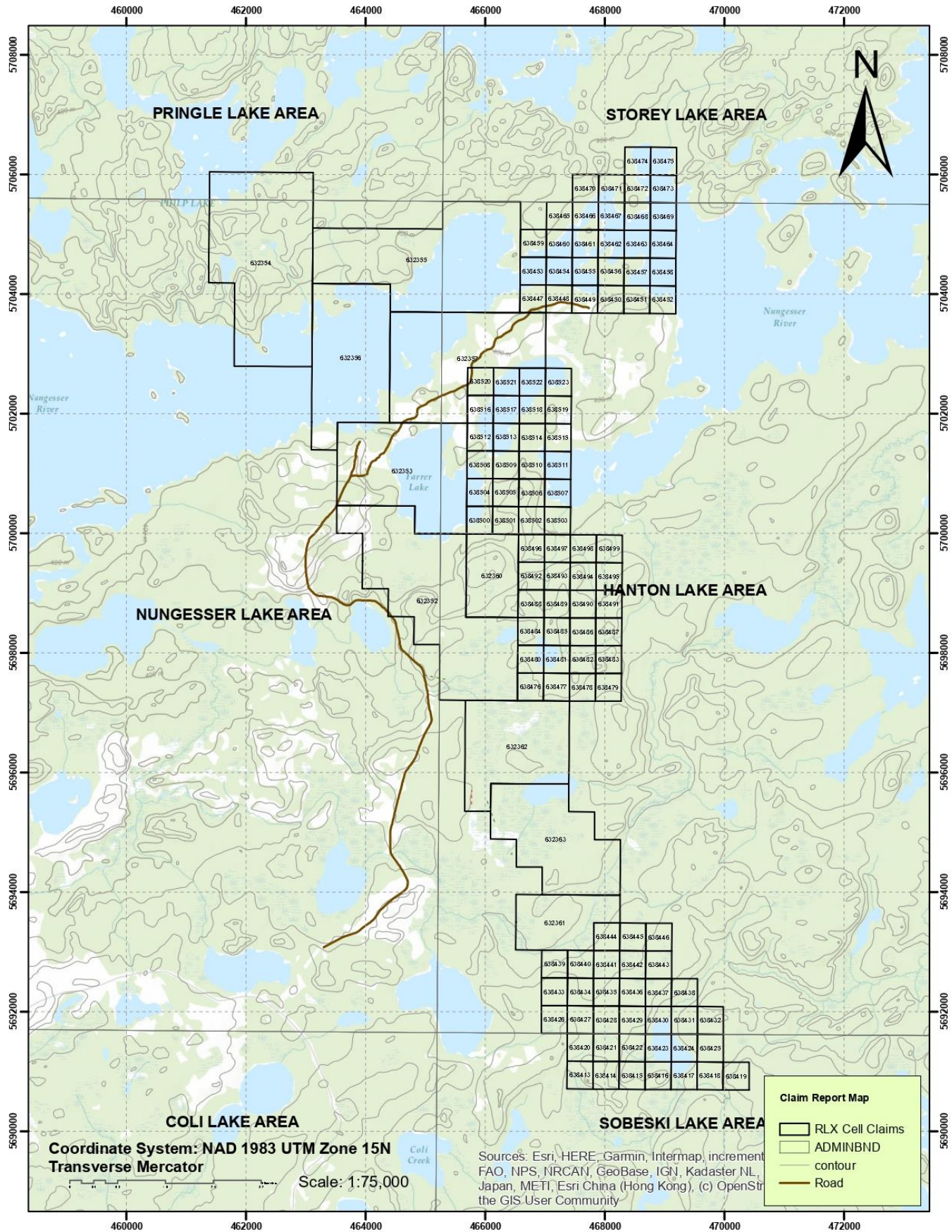


**Figure 2: RLX Claims**

ground and sandy areas. The Property is covered by unconsolidated glacial till and glacio-fluvial sand. There is limited outcrop exposure as a result of the extensive glacial overburden.

The climate of the area is sub-arctic / northern continental with a wide range of temperatures from lows of -40°C in winter to highs of +35°C in summer. Snow usually starts to fall in late October to early November and starts to melt in March. During the summer, the area experiences a moderate climate with periodic rain showers and can be impacted by atmospheric depressions centered on Hudson's Bay. The area has been subject to extensive forest fire activity in recent years and the mossy forest cover of substantial portions of the RLX Property has been affected.

The property is accessed via the Nungesser Road that intersects Hwy 125 near Balmertown (Figure 3). The following records directions from the intersection of the Nungesser Road with the Coli Road near kilometer 30 of the Nungesser Road where the Sidace gold exploration property is shown on Figure 3. Road names are recorded in the ODM roads and trails database. Take the Coli Road east of the intersection with the Nungesser Road for about 4 kilometers to the intersection with the Martene Road. Travel north on the Martene Road for about 10 kilometers to the intersection with the Sidace Road. Until 2021, truck travel was limited to about 2 kilometers past the Martene Road intersection and only ATV vehicles could travel past this point. In 2021, the Sidace Road was rehabilitated for vehicle travel, removing mostly deadfall and alder growth, making it possible to access the southern shoreline of Nungesser Lake. Stream crossings no longer have installed culverts and so are subject to erosion and may be impassable during times of high-water flow. The Sidace Road and ATV trails originating on the Sidace Road provide direct access to the property.

The property crosses Nungesser Lake towards its northern extent (Figure 2). Access to the northern shore of Nungesser Lake is provided by boat. For work conducted in 2021, boats were rented from the Nungesser Lake Lodge (Figure 3), which also provided lodgings.

## **5.0 HISTORY**

The RLX Property has had limited exploration activity in the past. Much of the work conducted in the area has been of regional scale for exploration target generation using geophysics, soil sampling, and some diamond drilling. Dome Exploration Ltd (1980) conducted more detailed geophysical surveys with follow-up diamond drilling and Rampart Ventures Ltd. conducted overburden sampling, geophysical surveys, geological mapping, and soil sampling over more than 50% of the RLX property between 2003 and 2005 (Bowdidge, 2005, Collins et al., 2005).



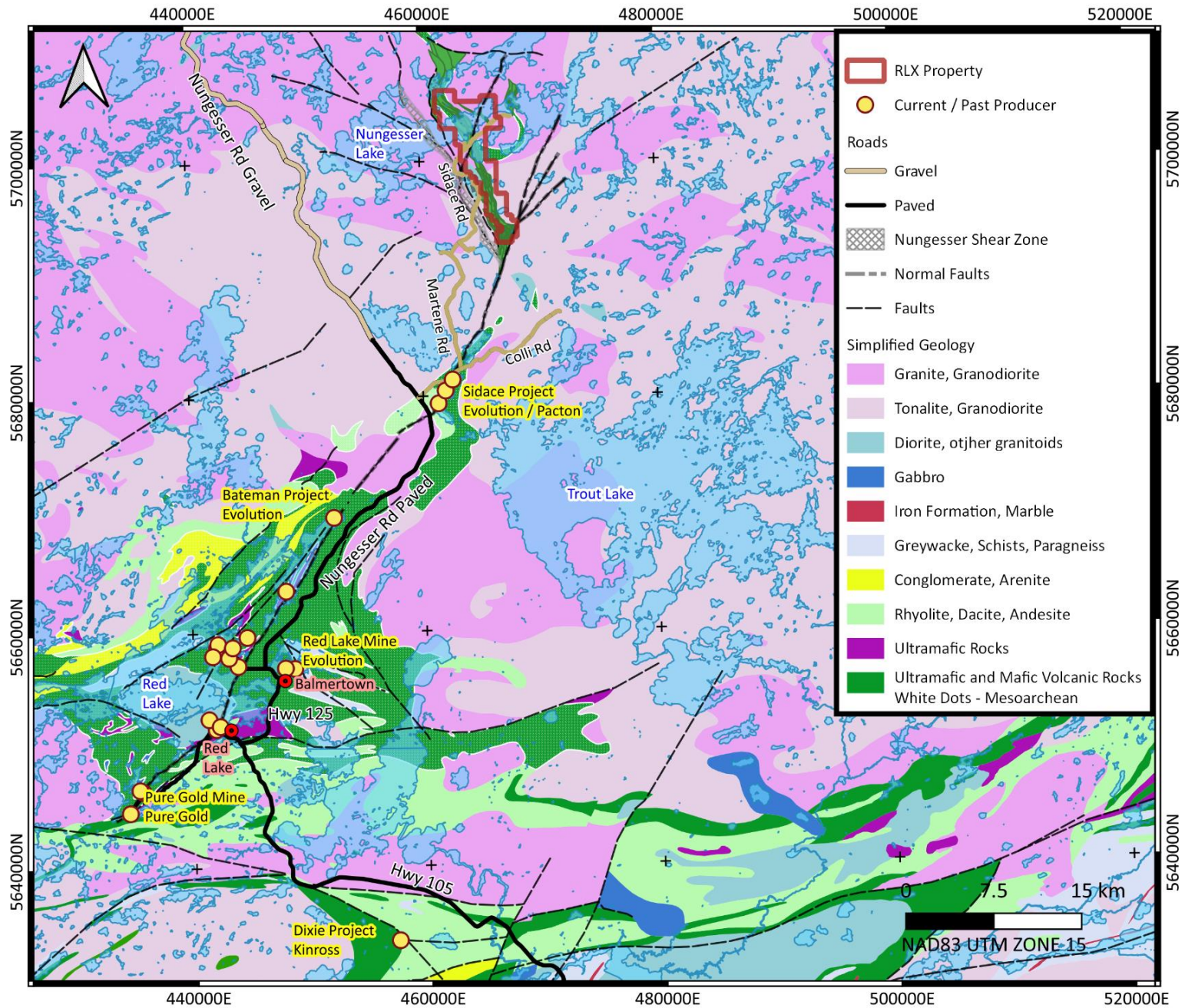


Figure 3: Red Lake Area, Regional Geology, Property Access



Dome Exploration Ltd. conducted an airborne magnetic survey in 1977 performed by Questor Surveys Ltd, using the input method (Pollock, 1978). This survey covered an area of 629 km<sup>2</sup> with a goal of targeting base metal occurrences. Dome Exploration Ltd. followed up on targets generated by airborne surveys with gridding and ground electromagnetic and magnetic surveys in 1988 (Bergmann 1978a, 1978b. Woodard 1979a, 1979b). In 1980, 11 drillholes were completed in the area targeting electromagnetic geophysical anomalies (Dome Exploration Ltd., 1980). Anomalous gold values are reported in two drill holes while in others trace gold values or no assays are reported. Most drill collars are plotted on Figure 4)

and details of the collars are listed in Table 3.

**Table 3: Dome Exploration Diamond Drilling**

HOLE_ID	_83UTM15E	_83UTM15N	ELEV_M	SIZE	DIP	AZ	OB	LENGTH	NTS_NUM	AREA	NOTE
122A-1	467797	5705048	401	AQ	-52	85	1.8	79.86	52N06NW	Hanton	
122A-1A	467846	5705093	398	AQ	-52	260	3.9	62.79	52N06NW	Hanton	
122A-2	467992	5704792	391	AQ	-51	80	7.9	177.70	52N06NW	Hanton	
122A-2A	468116	5704857	391	AQ	-59	265	17.9	100.89	52N06NW	Hanton	
122B-1	465899	5698527	429	AQ	-49	206	7.9	163.37	52N06NW	Hanton	
122B-2	467334	5697918	430	AQ	-48	90	6.4	118.87	52N06NW	Hanton	
122B-3	464810	5700367	393	AQ	-53	68	16.46	92.96	52N05NE	Nungesser	
122B-4	465108	5700432	393	AQ	-55	68	31.71	108.81	52N05NE	Nungesser	
122B-5	464404	5701886	396	AQ	-52	68	26.83	114.60	52N05NE	Nungesser	
122B-6	463724	5703738	392	AQ	-56	68	21.34	122.83	52N05NE	Nungesser	Anomalous Gold
122B-7	465495	5703770	391	AQ	-54	33	17.9	112.17	52N06NW	Hanton	Anomalous Gold
122B-8	464344	5704579	416	AQ	-53	33	4.57	83.52	52N05NE	Nungesser	
122C-1	467013	5692221	437	AQ	-51	62	21	144.17	52N06NW	Hanton	

NOTE: Collar locations modified from ODM DH database based on review of Dome Exploration Maps. Location, overburden (OB) and elevation in meters.

The maps of Stone and Good (1990) and Stone and Crawford (1994) cover the current RLX and adjacent properties to the west. They identified areas of undivided mafic rocks and greywacke near Nungesser Lake. They also identified a wide range of intrusive rocks including late intrusive bodies ranging from diorite to syenitic granite assigned to the regionally important Sanukitoid group. The Sanukitoid affinity of leucogabbro on the RLX property was confirmed by geochemical analysis performed by Lichtblau et al (2001). Sanukitoid suite intrusive rocks are observed near crustal scale structures and are

characterized by geochemistry indicating mantle derivation. During the winter of 2004, Rampart Ventures Ltd. subcontracted Terraquest Ltd. who flew an aeromagnetic survey on and near the RLX Property (Barrie, 2004). During the summer of the same year, they completed prospecting, geological mapping, soil sampling and ground geophysical surveys (Bowdidge, 2005) over about 60% of the RLX property at the time the SkyTEM survey was flown. Results of this mapping are discussed further below. Collins et al (2005) report on a trenching and soil sampling program also conducted for Rampart Ventures Ltd. The samples were obtained using an excavator and hand dug pits.

In 2008, an airborne geophysical dataset of magnetic and electromagnetic data was released that covers the greenstone enclaves (Ontario Geological Survey, 2008) described in Buse and Prefontaine (2007). The surveys provide a continuous high-resolution base for exploration in the area and mark many electromagnetic anomaly trends yet to be investigated. Some of the better electromagnetic responses are within the RLX claim group. Analysis of the data by a third-party geophysical consultant (in3D Geoscience Inc), concluded that a new heli-borne EM survey using current technology and tighter line spacing would address some of the high background issues and lack of detail identified within the 2008 OGS survey.

Recent geological mapping and rock sampling conducted for Pacton Gold Inc. is reported by Tims (2020) on adjoining claims directly west of the RLX Property. Various intermediate to felsic intrusive rock types were mapped and only a few supracrustal outcrops were noted.

Solstice acquired the RLX property in early 2021 and immediately flew a helicopter-borne magnetic survey over the property reported in Barham (2022). Based on the interpretation of this survey, including but not limited to, the identification of prominent NE-trending structures, the property was expanded over the summer of 2021. Recognition of important electromagnetic response in the 2008 Ontario Geological Survey airborne data prompted the commissioning of the SkyTEM survey reported here.

## **6.0 REGIONAL AND LOCAL GEOLOGY**

### **6.1 Regional Geology**

The property covers the southernmost of several known north-south trending greenstone enclaves in granitic rocks mapped by Stone and Good (1990), Stone and Crawford (1994) and partially by Buse and Prefontaine (2007). To the southwest of the property lies the Red Lake greenstone belt mapped in detail by Sanborn-Barrie et al (2004). Buse and Prefontaine (2004) assert that the Berens River greenstone remnants are the strike equivalent of Red Lake greenstone belt rocks.

The oldest rocks identified by Sanborn-Barrie et al (2004) are volcanic, intrusive, and lesser

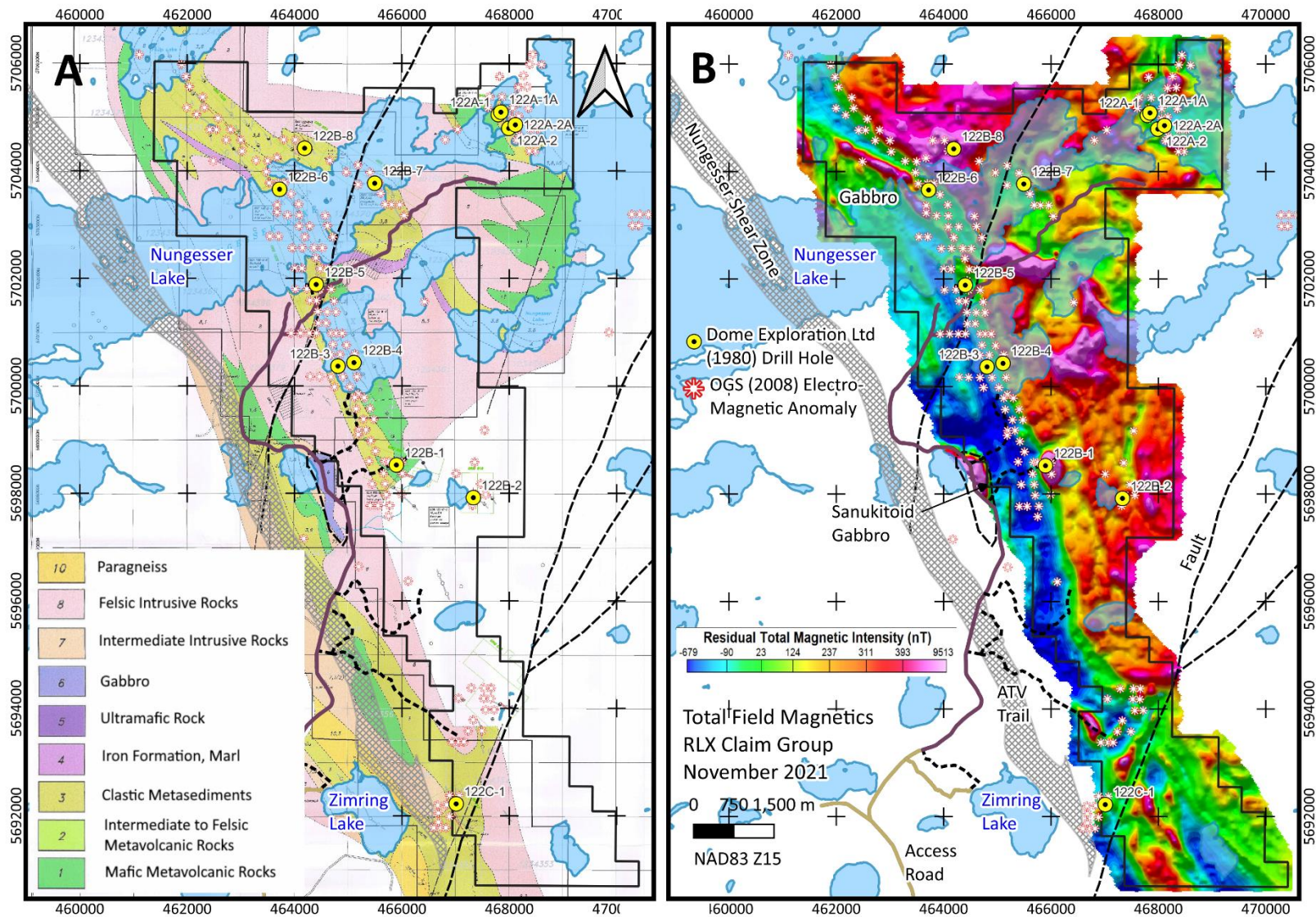


Figure 4: Bowdidge (2005) Geology 4B: Total Field Magnetic Results (2022: This Report)

sedimentary rocks of the Balmer Group (ca 2.98 Ga). An overlying sequence of ca 2.94 Ga volcanic, intrusive and sedimentary rocks is identified as the Ball Group and this age is consistent with the oldest volcanic ages reported by Buse and Prefontaine (2007). They also report both Mesoarchean and widespread Neoproterozoic granitic intrusive ages. The mapping of Bowdidge (2005) and Tims (2020) support a wide range of intrusive ages at the RLX property.

The Nungesser Deformation Zone (Figure 3) is a northwesterly striking zone of strongly foliated and locally mylonitized rocks with west dips of 50 to 80° (Stone and Good, 1990). Geophysical interpretation supports the extension of this deformation zone north to other Berens River supracrustal outcrop areas where structures identified in seismic section by Calvert et al (2004) are suspected to surface. The juxtaposition of major deformation zones, surfacing crustal scale extensional structures, and sanukitoid intrusive rocks provides a rich environment for gold exploration.

## **6.2 Local Rock Types and Structural Geology**

Bowdidge (2005) provides an outcrop map covering about 60% of the RLX claim group. On Figure 4, this map is compared to the total field magnetics acquired by SkyTEM for this survey. The claim group is marked by central magnetic low that corresponds with a narrow-deformed belt of meta-volcanic and meta-sedimentary rocks on the map of Bowdidge (2005). The metavolcanic rocks are amphibolites and intermediate to felsic fragmental rocks while the metasediments are clastic biotite gneiss to more mature arkose and quartzite. Small outcrops of chemical metasediments represented by oxide iron formation and marl are reported by Bowdidge (2005). Marl is also reported in drill hole 122-C1 which was completed near the southwest limit of the property by Dome Exploration (1980). Prominent magnetic highs correspond with gabbro bodies shown on the map of Bowdidge (2005) including a distinct anomaly associated with the Sanukitoid gabbro described in Litchblau et al (2001). Sanukitoid plutons are known host platinum group mineralization in the Superior Province of Ontario and are regarded as mantle-derived magmas which are associated with deep-tapping structures.

A northwest trending tectonite (Nungesser Deformation Zone, Figure 4) was mapped by Stone (1988) to the immediate west of the RLX property. The zone is described as a westerly dipping one-kilometer-wide area of schistose, mylonitized and fractured plutonic rocks. A hornblende tonalite body is described as having undergone a one-kilometer sinistral displacement within the zone (Stone, 1988). Bowdidge (2005) mapped these rocks and reports only a few tonalite outcrops exhibiting strong deformation fabrics and maps mature arkosic sediments where Stone (1988) reports tectonized granitoids.

Tims (2020) presents detailed mapping in the area reporting some sediments and some granitoids but also does not mention the Nungesser Deformation Zone. Stone (1998) places the development of major mylonite zones among the latest events in the local geologic history broadly coincident with the emplacement of mantle derived Sanukitoid plutons.

The RLX claim group occurs near the transition between the east-west trending Red Lake greenstone belt to the southwest and north-south trending Berens River greenstone slivers to the north. Sanborn-Barrie et al (2001) describe early north-south (D1) fabrics and folds and northeast – southwest crosscutting D2 fabrics and folds in the Red Lake greenstone belt. Stott et al (2001) report regionally consistent relationships in the Berens River greenstone slivers of D1 fabrics overprinted by D2 dextral shearing producing shallowly south plunging minor folds. Calvert et al (2004) describe an extensional regime interpreted from lithoprobe seismic data that is not reflected in studies of the Red Lake or Berens River greenstones.

Most structural measurements shown on the map of Bowdidge (2005) do not indicate dip direction and where they do, they tend to indicate steeply west dipping rocks. Most structural measurements reported by Tims (2020) indicate NNW-SSE striking foliation and steep westerly dips with some steep easterly dips. Sericite schists are known to mark structures in the area of the Sidace gold zones. A sericite schist has been intersected two drill holes of Dome Exploration Ltd (1980) in the central part of the RLX property suggesting a minimum strike of 1.6 km. Buse and Prefontaine (2007) assert that their mapping of greenstone slivers indicates predominantly east facing overturned west dipping rocks and their age, lithology and geochemistry can be directly correlated with the Red Lake greenstone belt. A comprehensive evaluation of the structure of the RLX property awaits further geological mapping.

### **6.3 Mineralization**

Solstice Gold Corp. acquired the RLX Property for its lode gold potential and believes the rock types and geophysical signature evident at the Sidace gold occurrences are likely present on the RLX Property. Dome Exploration Ltd (1980) reports drill intersected sericite schists, iron formation and skarn that are associated with gold mineralization in the Sidace area (Power-Fardy and Breede, 2009).

Dome Exploration Ltd (1980) completed thirteen diamond drill holes on or directly adjacent to the RLX property evaluating principally electromagnetic HLEM anomalies (Figure 4). Widespread pyrrhotite as exhalate layers or as secondary disseminations in intrusive rocks appear to be the source of the HLEM anomalies (Figure 4). Dome Exploration Ltd (1980) report anomalous gold values in DDH 122-B6 and DDH

122-B7 collared on the ice of Nungesser Lake (Figure 4). The anomalous gold values are reported from Quartz Diorite with concentrations of pyrrhotite in DDH 122-B6 and brecciated and silicified quartz feldspar porphyry in DDH 122-B7. Two holes (DDH 122-B3, 122-B5, Figure 4) drilled by Dome Exploration Ltd (1980) intersected intervals of sericite schist suggesting a minimum strike length of 1.6 km. Skarn (calc-silicate diopside bearing zones) is also important within the Sidace rocks and is reported in several logs from the Dome Exploration Ltd (1980) drilling. Skarn effects related to proximal granitic intrusions are reported within the Madsen Mine (Dube et al, 2000) and other gold deposits in the Red Lake area. An internal review of the Dome Exploration Ltd (1980) drilling suggests many of the holes failed to explain the anomalies they were targeted to intersect.

Electromagnetic anomalies reported in the OGS (2008) airborne survey are shown on Figure 4 and support correlation with the Sidace area where electromagnetic anomalies assist in the interpretation of buried stratigraphy. Electromagnetic response acquired during this SkyTEM survey are detailed below.

## **7.0 EXPLORATION**

Exploration of the property is limited to the historical description provided above. Solstice completed a helicopter borne magnetic survey in February of 2021 reported in Barham (2022). This subsequent electromagnetic survey reported in Appendix B, includes gridded data for total field and derivative magnetic data, a digital elevation model, and multi-channel time domain results. Additionally, conductivity-depth slices derived from inverted data are included in Appendix B. A brief discussion of results follows.

The SkyTEM report (Appendix B) describes the survey instrumentation and data processing in detail. Table 3 provides some details of the survey design and delivered data products.

The SkyTEM system is a time domain survey that transmits both a High Moment and Low Moment current (Table 3) in pulses. When the transmitter is off the receivers record details of secondary eddy currents induced by the transmitted current. Stronger induced currents are generated by conductive bodies. High Moment transmission can induce secondary currents in deeper bodies. The data are collected by the receiver within time windows (Gates) that can be correlated to characteristics of an induced secondary field. Figure 5 shows an example of a low moment and high moment result. Conductive bodies are associated with interpreted supracrustal rocks. Lake effect conductivity is apparent in the low moment data (LM). This data is being evaluated by Solstice Gold Corp.

SkyTEM also completed a data inversion processing task for Solstice Gold Corp that calculated a

three-dimensional model of conductivity from the EM data. The calculation is detailed in the report in Appendix B. Figure 6 shows two depth-conductivity slices from this work at minus 50 meters and minus 260 meters. Other slices are included in Appendix B. The model shows stronger conductivity at depth. This model is being evaluated by Solstice Gold Corp.

**Table 4: SkyTEM Survey Details**

<b>Full Survey Statistics (See report Appendix B)</b>		
<b>Contractor: SkyTEM Surveys ApS</b>		<b>Survey Flown Nov 5-15 2021</b>
Survey Size	879.1	Line Km
Direction	Az 90/270	Line Azimuths – NS Tielines
Line Spacing	75	meters
Terrain Clearance	40	35-45 meters
Airspeed	100	90-110 Km/hr nominal production speed
High Moment Current	108.3	Amp - HM EM data products
Low Moment Current	5.8	Amp - LM EM data products
Instrument Location	m	3 Digital GPS units
DEM Product	m	Instrument location - laser altimeter
Magnetic Base Stn	nT	Red Lake Airport
<b>Data Products (See report Appendix B)</b>		
Flight Paths	RLXStem_Flight_Path_UTM15N.pdf	
DEM	RLXStem_DEM_UTM15N.pdf	
Electromagnetic Noise	RLXStem_PLNI_UTM15N.pdf	
Total Field Magnetics	RLXStem_MAG_TMI_UTM15N.pdf	
High Moment EM	RLXStem_HMZ_UTM15N.pdf (All gates)	
Low Moment EM	RLXStem_LMZ_UTM15N.pdf (All gates)	
Conductivity Depth	RLXStem_Con_DOI_Depth_Plots.pdf (all slices)	

## 8.0 INTERPRETATION

Supracrustal rocks correspond to a north northeast-south southwest trending magnetic low continuous over the 14.5 km extent of the airborne magnetic survey. These results are being evaluated by Solstice Gold Corp. Conspicuous magnetic highs can be correlated with gabbro bodies mapped by Bowdidge (2005) and one of which corresponds to a mantle derived Sanukitoid pluton potentially marking the location of a crustal scale deformation zone. Smaller faults are recognized in the magnetic results as lineaments that truncate and offset magnetic anomalies. Some of these could be strike equivalents of structures important within gold zones to the southwest.

Electromagnetic anomalies reported by the Ontario Geological Survey (2008), are confirmed by the SkyTEM survey and define layer parallel anomalies predominantly within this magnetic low. An inversion



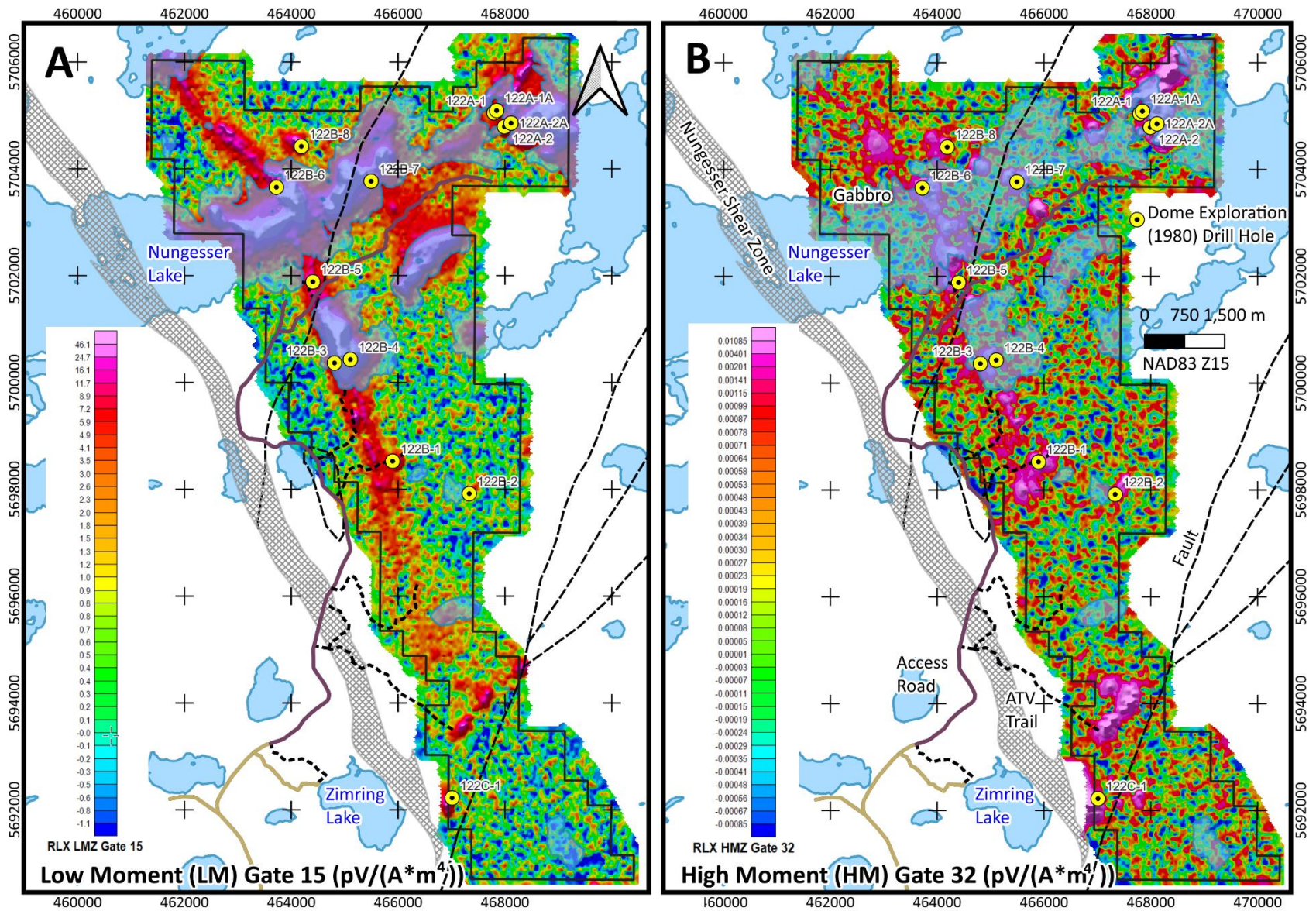


Figure 5A: Low Moment (LM) Gate 15 Conductivity 5B: High Moment (HM) Gate 32 Conductivity



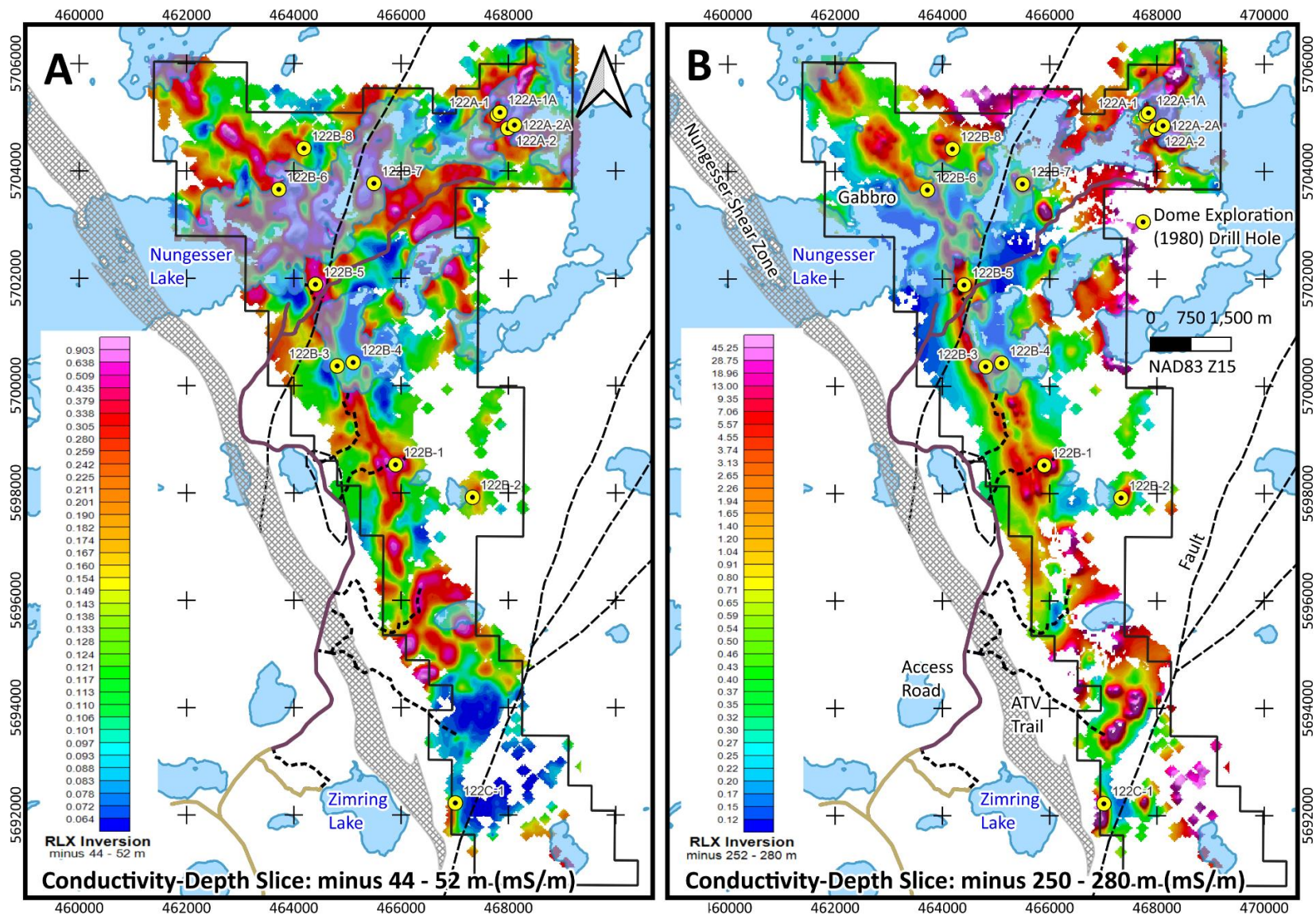


Figure 6A: Conductivity – Depth minus 50m 6B: Conductivity – Depth minus 260 m

model of the electromagnetic results suggest conductive response is stronger at depth. Near surface responses suggest the presence of an airborne IP effect (“AIP”) which may affect the SkyTEM EM model. These results and possible effects of AIP are being evaluated by Solstice Gold Corp.

**9.0 RECOMMENDATIONS**

Ground geological mapping and prospecting are recommended to aid in the development of a comprehensive exploration program. Along with prospecting and mapping, a test soil survey should be conducted to evaluate the effectiveness of this technique. Based on the results of these programs drilling of identified targets should be carried out.

**Table 5: Recommended Future Work**

<b>Work Program</b>	<b>Approximate Cost (\$CDN)</b>
Prospecting & Mapping Program	\$200,000
Soil Survey	\$30,000
<b>TOTAL</b>	<b>\$230,000</b>

## 10.0 REFERENCES

- Barham, B.A., 2022.** RLX Property, Helicopter Borne Airborne Magnetic Survey, Red Lake Area, Ontario. Report prepared for Solstice Gold Corp,
- Bergman, H.J., 1978a.** Report on Geophysical Survey for Dome Exploration (Canada) Ltd., Project I22B, Northred, Ontario in MNDM Assessment File 2.3000.
- Bergman, H.J., 1978b.** Report on Geophysical Survey for Dome Exploration (Canada) Ltd., Project 122C, Northred, Ontario in MNDM Assessment File 2.3066.
- Bowdidge, C., (2005):** Report on the 2004 Exploration Program for Rampart Ventures & Inlet Resources Ltd. on the North Red Lake Property – Nungesser-Trout Lakes Area, 87 p, MNDM Assessment file 20000000582.
- Buse, S. and Préfontaine, S. 2007.** Precambrian geology of the McInnes Lake greenstone belt, the supracrustal remnants study area and the Frame Lake pluton, Berens River Subprovince, Ontario; Ontario Geological Survey, Open File Report 6210, 128p.
- Calvert A.J., Cruden A.R. and Hynes A., (2004):** Seismic evidence for preservation of the Archean Uchi granite–greenstone belt by crustal-scale extension, *Tectonophysics* 388 (2004) 135– 143.
- Collins, P.A. & Averill, S.A., 2005.** Rampart Ventures Ltd., North Red Lake Project, Ontario, Canada, Report on Overburden Trenching and Heavy Mineral Sampling for Gold.
- Dome Exploration Ltd. (1980):** Diamond Drill Hole Logs listed in the Ontario Department of Mines Diamond Drill Hole repository.
- Dubé, J., (2021):** High-Resolution Heliborne Magnetic Survey RLX Property, Nungesser Lake Area Red Lake Mining Division, Ontario, 2021 – This Report, Appendix B.
- Dubé, B., Balmer, W., Sanborn-Barrie, M., Skulski, T., and Parker, J., 2000:** A preliminary report on amphibolite-facies, disseminated-replacement-style mineralization at the Madsen gold mine, Red Lake, Ontario; Geological Survey of Canada, Current Research 2000-C17
- Lichtblau, A., Raoul, A., Ravnaas, C., Storey, C.C., Kosloski, L., Debicki, R. and Drost, A. (2001):** Report of Activities 2000, Resident Geologist Program, Red Lake Regional Resident Geologist Report: Red Lake and Kenora Districts; Ontario Geological Survey, Open File Report 6047, 109p.
- Ontario Geological Survey, 2008.** Ontario airborne geophysical surveys, magnetic and electromagnetic data, halfwave data (compressed ASCII format) and calibration data, Whitefeather Forest area, GEOTEM®1000 survey; Ontario Geological Survey, Geophysical Data Set 1058b.
- Pollock, F. W., t 978.** Airborne Magnetic Survey, Dome Exploration (Canada) Ltd., Trout Lake Area in MNDM Assessment File 2.2636.
- Power-Fardy D. and Breede K., 2009:** Technical Review of the Sidace Lake Gold Property, including Mineral Resource estimate for the Main Discovery and Upper Duck Zones, Red Lake Mining Division, Northwestern Ontario, 43-101 technical report prepared for Planet Exploration Inc. by Watts, Griffis and McOuat.

**Sanborn-Barrie, M., Skulski, T., and Parker, J., 2004:** Geology, Red Lake greenstone belt, western Superior Province, Ontario; Geological Survey of Canada, Open File 4594, scale 1:50,000.

**Stone, D., 1988;** Project Number 88-34: Geology of Berens Subprovince: Nungesser Lake Area, District of Kenora, *in* - Summary of Field Work and Other Activities 1988, Ontario Geological Survey Miscellaneous Paper 141, pp 75-80.

**Stone, D., 1998,** Precambrian Geology of the Berens River Area, Northwest Ontario. Ontario Geological Survey. Open File Rept. 5963.

**Stone and Crawford, 1994,** Precambrian geology, Henfrey Lake area, Ontario Geological Survey, Preliminary Map P3278, scale 1:50,000

**Stone and Good, 1990,** Precambrian geology, Nungesser Lake, Ontario Geological Survey, Preliminary Map P3175, scale 1:50,000

**Tims, A., 2020,** Geological Mapping and Prospecting on the Golden Loon Property, Red Lake Mining District, Ontario November 5th, 2020, report prepared for GoldSpot Discoveries Corp.

**Woodard, J.A., 1979a,** EM and Magnetic Survey for Dome Exploration (Canada) Ltd., Project 122B South, Northred in MNM Assessment File 2.3002.

**Woodard, J.A., 1979b,** EM and Magnetic Survey for Dome Exploration (Canada) Ltd., Project 122A, Northred in MNM Assessment File 2.3064.

## **APPENDIX A: Statement of Qualifications**

**June 13, 2022**

I, Bruce Alexander Barham, do hereby certify that:

- 1 – I hold a Bachelor of Science, Honours in Geology from the University of Manitoba (1984) and a Master of Science, Geology from Carleton University, Ottawa, Ontario, 1987.
- 2 – I am a Professional Geoscientist (PGO number 3406) registered with the Professional Geoscientists of Ontario.
- 3 – I am employed by Solstice Gold Corp. whose head office is Suite 550 - 800 West Pender Street Vancouver, BC, Canada, V6C 2V6
- 4 – I am the author of this Technical Report on the RLX Property, Red Lake, Ontario.
- 5 – I supervised the work reported on in this report.
- 6 – This report is complete and correct to the best of my knowledge.

Signed,



---

Bruce A. Barham, PGO  
Senior Geologist  
Solstice Gold Corp.  
Calgary, Alberta

**APPENDIX B: Report**

**SkyTEM Heliborne Electromagnetic Survey  
RLX Property, Nungesser Lake Area  
Red Lake Mining Division, Ontario, 2021  
Technical Report January 2022**

**Map Products**

# DATA REPORT

## **SkyTEM Survey: Red Lake, Ontario, Canada**

Client: Solstice Gold

Date: January 2022





## Structure of the Digital Data Delivery catalogue

Folder	Sub folder	Sub folder	File format	Content
01_Data	01_GDB		.gdb (Geosoft)	Data
02_Inversion	01_GDB		.gdb (Geosoft)	Modelled layer conductivity
	02_Layer_conductivity_Grids		.grd (Geosoft grids) .TIFF	Modelled layer conductivity
	03_Layer_conductivity_Maps		.map (Geosoft maps) .pdf	Modelled layer conductivity
	04_Sections		.png	Profile sections of modelled layer conductivity & model analysis
03_Maps	01_DEM		.map (Geosoft maps)	DEM
	02_FlightPath			Flown lines
	03_PlannedSurveyLines		.pdf	Survey outline
	04_MAG			MAG (RMF & TMI)
	05_EM			EM (dB/dt)
	06_PLNI			PLNI
04_Grids	01_DEM		.grd (Geosoft grids)	DEM
	02_EM	01_LM_Z 02_HM_Z	.grd (Geosoft grids)	Height Corrected EM Z channels
	03_MAG		.grd (Geosoft grids)	MAG
	04_PLNI		.grd (Geosoft grids)	PLNI
05_Report			.pdf	Report

# Contents

Contents .....	3
Executive Summary.....	4
Introduction .....	5
Survey outline.....	6
Flight Parameters .....	9
Flight Reports.....	10
Instruments .....	12
Airborne unit.....	12
Ground base stations .....	13
Data Acquisition .....	14
Gate times.....	14
Waveform .....	17
Digital Data .....	20
Inversion results.....	21
Data processing and presentation.....	22
Auxiliary data.....	22
Magnetic data.....	25
EM data .....	28
Power Line Noise Intensity (PLNI) .....	31
Inversion .....	33
References .....	39
Appendix list.....	40
Appendix 1: Instruments .....	40
Appendix 2: Introduction to Spatially Constrained Inversion (SCI) .....	40

# Executive Summary

This report covers data acquisition, technical specifications, data processing and presentation of the SkyTEM312M survey flown in the period from November 5th to November 15th, 2021 northeast of Red Lake, Ontario, Canada.

The survey is comprised of 1 block containing a total of 879.1 planned flight lines.

The SkyTEM312M system collects time domain electromagnetic and magnetic data along with supporting navigation measurements.

All materials are delivered digitally; the final product includes:

- Data report
- Processed data in Geosoft database file format
- Inversion results; modelled layer conductivity in Geosoft database file format
- Grids and maps in Geosoft format
- Presentations of data and inversion results in png and/or pdf format

An overview of the digital data delivery can be seen on the first page in the report.

# Introduction

The SkyTEM electromagnetic and magnetic survey described in this report is flown with the SkyTEM312M system. The survey was requested by Solstice Gold and performed by SkyTEM. Basic survey information and key personnel are listed in Table 1.

This report covers data acquisition, instrument descriptions, data processing and presentations. The data delivery includes processed electromagnetic data and presentations, spatially constrained inversion results (SCI) and model presentations as well as processed magnetic data and presentations. The digital data delivery folder is described in the front inside cover of this report.

This report does not include any geological interpretations of the geophysical dataset.

<b>Solstice Gold (Client)</b>	
Client Contact person	Mr Mike Timmins mtimmins@solsticegold.com
<b>SkyTEM Surveys ApS (Contractor)</b>	
Project Manager	Mr Doug Garrie Email: dga@skytem.com
Field Crew	Mr Dominic Leblanc Mr Fred Ladouceur
<b>Expedition Helicopters (Helicopter operator)</b>	
Helicopter type	Eurocopter Astar 350 B3
Pilots	Mr Nick Greenfield
Data acquisition period	November 5th to November 15th, 2021
Data processing, presentations, and report	Mr Thomas Steensen

*Table 1 Key personnel and survey information.*

## Survey outline

The survey area is located northeast of, Red Lake, Ontario, Canada. The planned survey lines (presented as blue lines on Figure 1) have a line spacing of 75 m in an E - W direction and tie lines with spacing 750 m in a N - S direction (Flight line details are listed in Table 2 and Table 3). The survey was flown from November 5th to November 15th, 2021.

Actual flown lines (red lines) are presented in Figure 2. Discrepancies between planned and flown lines can occur where difficult terrain or cultural features such as roads, buildings or powerlines necessitated a diversion from the planned lines.

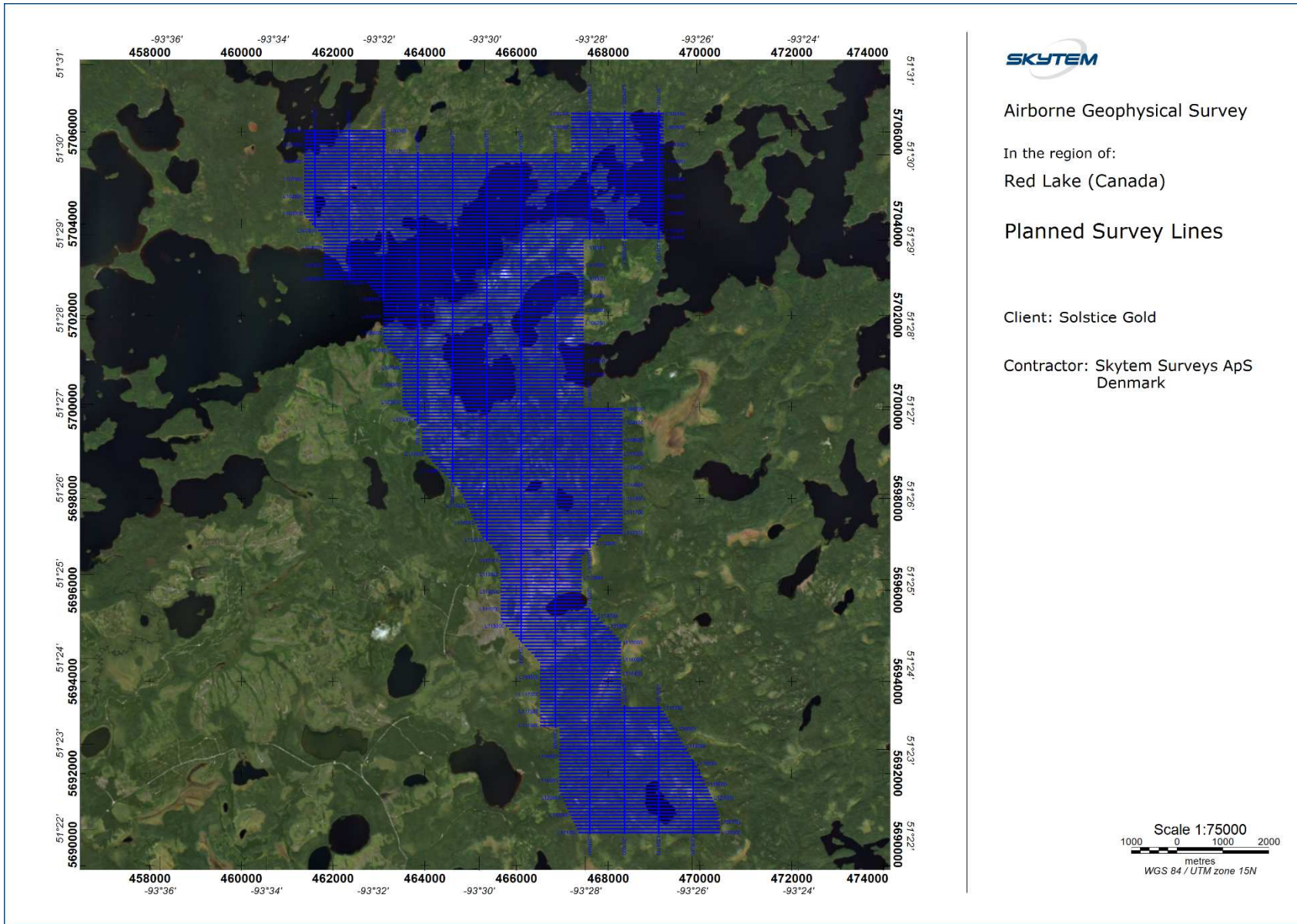
The coordinate system UTM Zone 15 N (WGS84) was used throughout this report, and in the data delivery.

Name	Spacing m (in- /tie line)	Direction (in- /tie line)	Number of Lines	Total km
Red Lake	75 / 750	90° / 0°	217/16	879.1
<b>In Total</b>				879.1

*Table 2 Survey details*

Area	Line numbering
Red Lake	L100100 – L121000 / T200100 – T201200

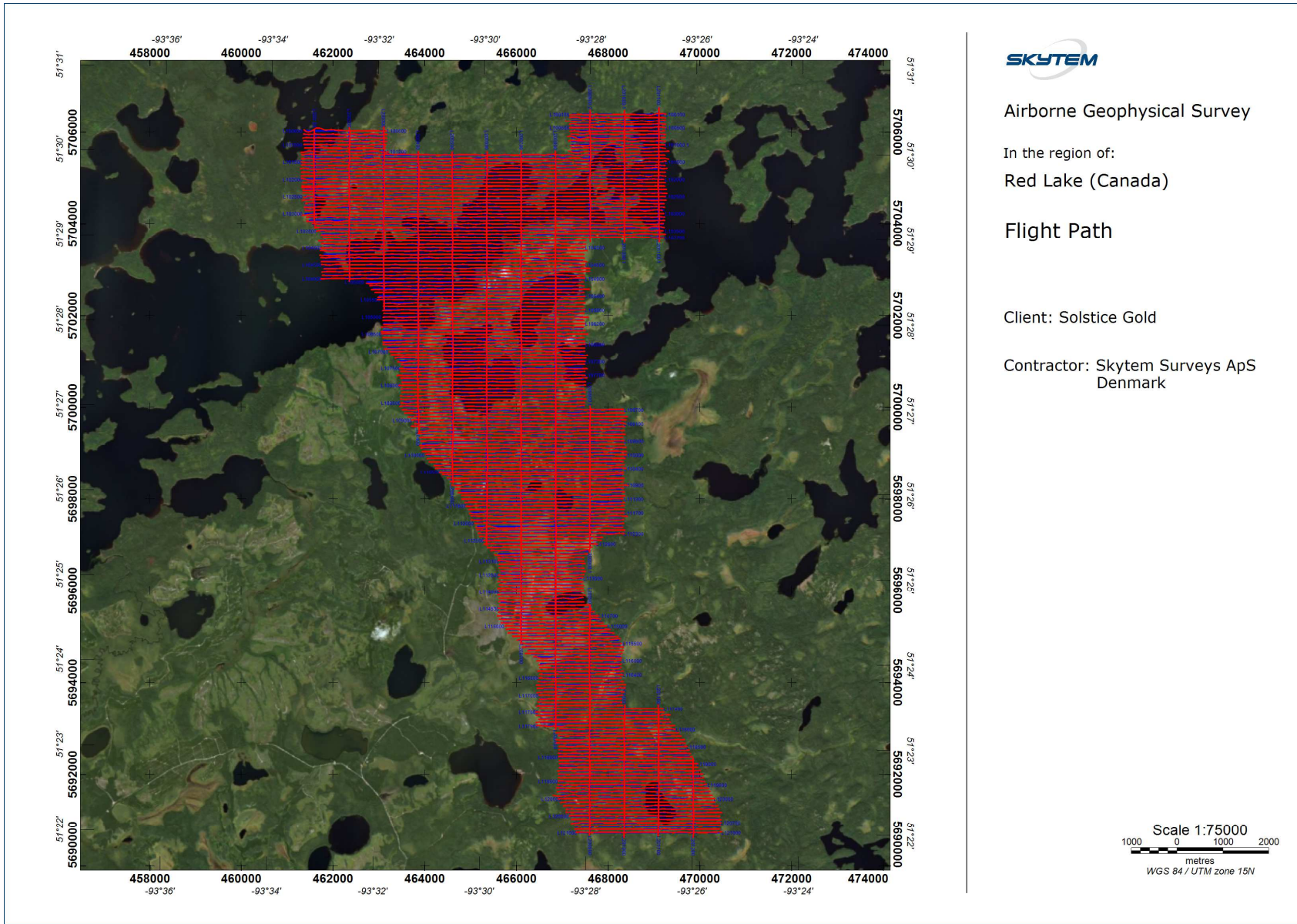
*Table 3 Line numbering*



2022/01/13

Figure 1. Planned survey lines in blue.





2022/01/13

Figure 2. Actual flown lines in red superimposed on planned lines in blue.

## Flight Parameters

The nominal terrain clearance of the transmitter is 35-45 m, with an increase over forests, power lines, or any other obstacles or hazards. The safe flying height during the survey is always based on the pilot's assessment of risk and deviations from nominal values are at the discretion of the pilot.

The nominal production airspeed was 90-110 kph for a flat topography with no wind. This may vary in areas of rugged terrain and/or windy conditions.

Average values and standard deviations of survey flight parameters are found in Table 4.

Control parameter		Average Value	Standard Deviation
Ground speed*)		94.2 kph	11.9 kph
Processed height		52.6 m	9.0 m
Tilt angle	X	1.1 degrees	2.4 degrees
	Y	-0.7 degrees	1.1 degrees
High Moment Current		108.3 Amp	1.7 Amp
Low Moment Current		5.8 Amp	0.01 Amp

*Table 4 Flight parameters*

*\*) Actual speed varies as a function of day and flight direction due to different wind directions and magnitude.*



## Flight Reports

For each flight, a report with key information regarding the data acquisition is made in the field. Listed in the reports are details on the weather, special data parameters and other events which may influence the data. Weather report and flight report can be seen in Table 5 and Table 6, respectively.

Flight	Temperature (°C)	Wind (m/s)	Visibility
20211103.01	0	3	Good
20211103.02	2	4	Good
20211103.03	3	4	Good
20211103.04	4	4	Good
20211105.01	6	2	Ok
20211106.01	6	4	Good
20211108.01	2	5	Good
20211108.03	5	8	Good
20211109.01	2	6	Good
20211109.02	5	8	Good
20211110.01	-7	2	Good
20211113.01	-4	2	Good
20211114.01	-6	4	Good
20211114.02	-4	3	Good
20211115.01	-10	1	Good
20211115.02	-3	3	Good

*Table 5 Weather report*

Flight	Comments
20211103.01	Calibration
20211103.02	Calibration
20211103.03	Calibration
20211103.04	High Altitude Calibration
20211105.01	Production
20211106.01	Production
20211108.01	Production
20211108.03	Production
20211109.01	Production
20211109.02	Production
20211110.01	Production
20211113.01	Production
20211114.01	Production.
20211114.02	Production
20211115.01	Production
20211115.02	Production

*Table 6 Flight report.*

## Instruments

This section provides an overview of airborne as well as ground base instruments, thorough technical descriptions are provided in Appendix 1.

### Airborne unit

The airborne instrumentation comprising a SkyTEM312M system includes a time domain electromagnetic system, a magnetic data acquisition system and an auxiliary data acquisition system containing two inclinometers, two altimeters and three DGPS'. All instruments are mounted on the frame suspended ~40 m below the helicopter, the generator used to power the transmitter is suspended between the frame and the helicopter, ~30 m below the helicopter. A picture of the airborne SkyTEM312M unit is seen on Figure 3, and a sketch of the instrumentation is seen on Figure 4.



*Figure 3 SkyTEM312M Airborne unit.*

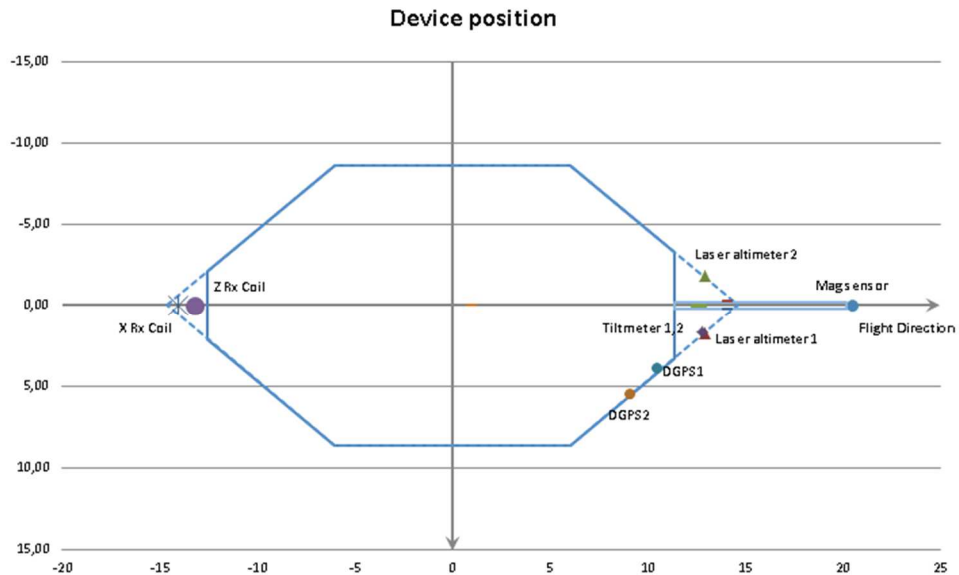


Figure 4 Sketch showing the frame and the position of the basic instruments. The blue line defines the transmitter loop. The horizontal plane is defined by  $(x,y)$ .

## Ground base stations

The DGPS and magnetic base stations were positioned in the vicinity of the landing site.

### DGPS base station

Backup DGPS base stations were placed at a location of maximum possible view to satellites and away from metallic objects that could influence the GPS antenna.

GPS processing involves a Precise Point Positioning (PPP) setup using the L2 band of the GPS rover. The PPP process eliminates the need of base station data and the improved precision obtained during the post-processing is based on correction and precision files which can be downloaded during the processing steps.

DGPS base station data is only acquired for backup and was not used in the processing on this survey.

### Magnetometer base station

The base station magnetometer was placed in a location of low magnetic gradient, away from electrical transmission lines and moving metallic objects, such as motor vehicles and aircrafts.

Locality	Latitude	Longitude	Height	Base Mag Constant (nT)
Red Lake Airport	51.0658°	-93.7944°	371 m	56881.6

## Data Acquisition

The SkyTEM312M system setup is a dual moment configuration containing a High Moment (HM) with a peak moment of  $\sim 500,000$  NIA and a Low Moment (LM) with a peak moment of  $\sim 3,000$  NIA.

Data from two DGPS receivers are recorded by the EM data acquisition system while a third DGPS is recorded by the magnetic data acquisition system. The DGPS systems are used for time stamping, positioning, and correlation of the EM and magnetic datasets. All recorded data are marked with a time stamp used to link the different data types.

The time stamp is in UTC/GMT and the formats are either,

- Date and Time defined as; yyyy/mm/dd hh:mm:ss.sss  
or
- Datetime values defined as decimal days since 1900-01-01; dddd.ssssssss

## Gate times

Raw and calibrated gate times for low moment and high moment are presented in *Table 7* and *Table 8*, respectively. All times are referred to start of turnoff of ramp down.

Calibration parameters for

Low Moment

Shift factor: 0.94 (on the raw dB/dt data)

Time shift:  $-1.99e-6$  s

High Moment

Shift factor: 0.99 (on the raw dB/dt data)

Time shift:  $-1.8e-6$  s

Note that the HM gate times are shifted  $350 \mu\text{s}$  in addition to the time shift of  $-1.8e-6$ s with respect to start of turnoff ramp, to move the gates away from the ramp.

HM effective calibrated gate center times (GCT\_cal):

$$\text{GCT\_cal} = \text{GCT} + \text{HM\_shift} - \text{time shift}$$

If third party processing or inversions are undertaken using the processed data (Geosoft GDB) as the base dataset, the calibrated gate center times found in Table 7 and Table 8 for LM and HM, respectively, must be applied.

Aarhus Workbench handles time shift and calibrations automatically as they are defined in the geometry file (.gex).

Gate #	GateOpen (μs)	Gate Close (μs)	Gate width (μs)	Raw Gate center (μs)	Calibrated LM Gate Center Time (μs)	Comment
1	0.43	1.00	0.57	0.715	-1.275	Not Used
2	1.43	3.00	1.57	2.215	0.225	Not Used
3	3.43	5.00	1.57	4.215	2.225	Not Used
4	5.43	7.00	1.57	6.215	4.225	Not Used
5	7.43	9.00	1.57	8.215	6.225	Not Used
6	9.43	11.00	1.57	10.22	8.225	Not Used
7	11.43	13.00	1.57	12.22	10.225	Not Used
8	13.43	16.00	2.57	14.72	12.725	Not Used
9	16.43	20.00	3.57	18.22	16.225	LM
10	20.43	25.00	4.57	22.72	20.725	LM
11	25.43	31.00	5.57	28.22	26.225	LM
12	31.43	39.00	7.57	35.22	33.225	LM
13	39.43	49.00	9.57	44.22	42.225	LM
14	49.43	62.00	12.57	55.72	53.725	LM
15	62.43	78.00	15.57	70.22	68.225	LM
16	78.43	98.00	19.57	88.22	86.225	LM
17	98.43	123.00	24.57	110.72	108.725	LM
18	123.43	154.00	30.57	138.72	136.725	LM
19	154.43	194.00	39.57	174.22	172.225	LM
20	194.43	245.00	50.57	219.72	217.725	LM
21	245.43	308.00	62.57	276.72	274.725	LM
22	308.43	389.00	80.57	348.72	346.725	LM
23	389.43	490.00	100.57	439.72	437.725	LM
24	490.43	617.00	126.57	553.72	551.725	LM
25	617.43	778.00	160.57	697.72	695.725	LM
26	778.43	980.00	201.57	879.22	877.225	LM
27	980.43	1235.00	254.57	1107.72	1105.725	LM
28	1235.43	1557.0	321.57	1396.215	1394.225	LM

Table 7 Gate times for the Low Moment.



Gate #	GateOpen (μs)	Gate Close (μs)	Gate width (μs)	Raw Gate center (μs)	Calibrated HM Gate Center Time (μs)	Comment
1	0.43	1.00	0.57	0.715	348.915	Not Used
2	1.43	3.00	1.57	2.215	350.415	Not Used
3	3.43	5.00	1.57	4.215	352.415	Not Used
4	5.43	7.00	1.57	6.215	354.415	Not Used
5	7.43	9.00	1.57	8.215	356.415	Not Used
6	9.43	11.00	1.57	10.215	358.415	Not Used
7	11.43	13.00	1.57	12.215	360.415	Not Used
8	13.43	16.00	2.57	14.715	362.915	Not Used
9	16.43	20.00	3.57	18.215	366.415	Not Used
10	20.43	25.00	4.57	22.715	370.915	Not Used
11	25.43	31.00	5.57	28.215	376.415	Not Used
12	31.43	39.00	7.57	35.215	383.415	Not Used
13	39.43	49.00	9.57	44.215	392.415	Not Used
14	49.43	62.00	12.57	55.715	403.915	Not Used
15	62.43	78.00	15.57	70.215	418.415	Not Used
16	78.43	98.00	19.57	88.215	436.415	HM
17	98.43	123.00	24.57	110.715	458.915	HM
18	123.43	154.00	30.57	138.715	486.915	HM
19	154.43	194.00	39.57	174.215	522.415	HM
20	194.43	245.00	50.57	219.715	567.915	HM
21	245.43	308.00	62.57	276.715	624.915	HM
22	308.43	389.00	80.57	348.715	696.915	HM
23	389.43	490.00	100.57	439.715	787.915	HM
24	490.43	617.00	126.57	553.715	901.915	HM
25	617.43	778.00	160.57	697.715	1045.915	HM
26	778.43	980.00	201.57	879.215	1227.415	HM
27	980.43	1235.00	254.57	1107.715	1455.915	HM
28	1235.43	1557.00	321.57	1396.215	1744.415	HM
29	1557.43	1963.00	405.57	1760.215	2108.415	HM
30	1963.43	2474.00	510.57	2218.715	2566.915	HM
31	2474.43	3120.00	645.57	2797.215	3145.415	HM
32	3120.43	3912.00	791.57	3516.215	3864.415	HM
33	3912.43	4880.00	967.57	4396.215	4744.415	HM
34	4880.43	6065.00	1184.57	5472.715	5820.915	HM
35	6065.43	7517.00	1451.57	6791.215	7139.415	HM
36	7517.43	9293.00	1775.57	8405.215	8753.415	HM
37	9293.43	11473.0	2179.57	10383.21	10731.415	HM

Table 8 Gate times for the High Moment.

## Waveform

The waveform is measured using the 60 Hz script applied for this survey.

The waveform is measured using a current probe (turn-on ramp) and a pick-up coil (outputs  $dI/dt$ ) for the turn-off ramp. The approximation to the measured waveform is applied in modelling of the EM data. Figure 5 and Figure 6 show the approximated up and down ramp and waveform details are presented in Table 9 to Table 12

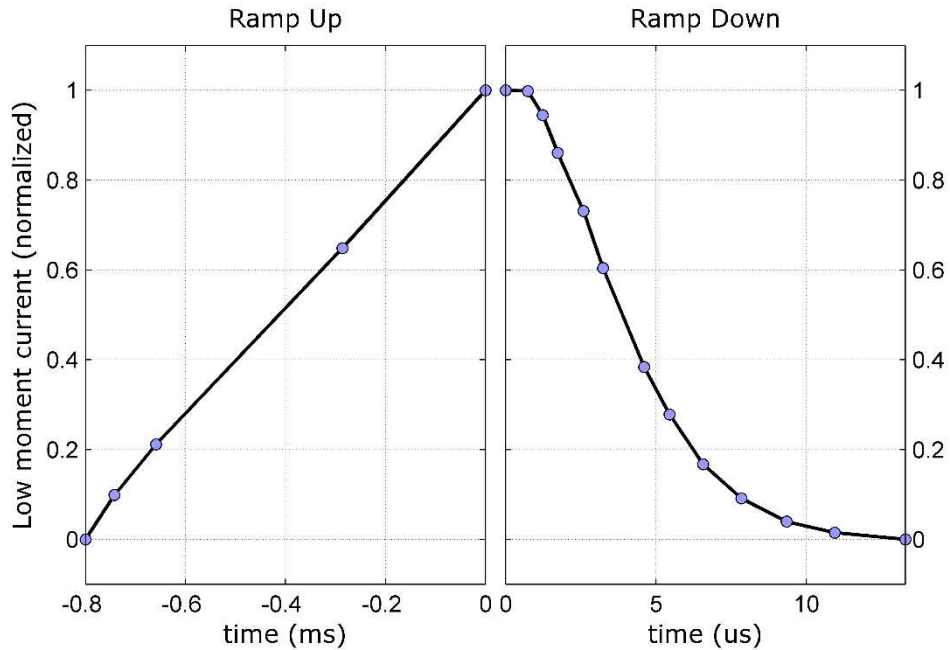


Figure 5. Ramp up and down for the LM waveform. The current is normalised.

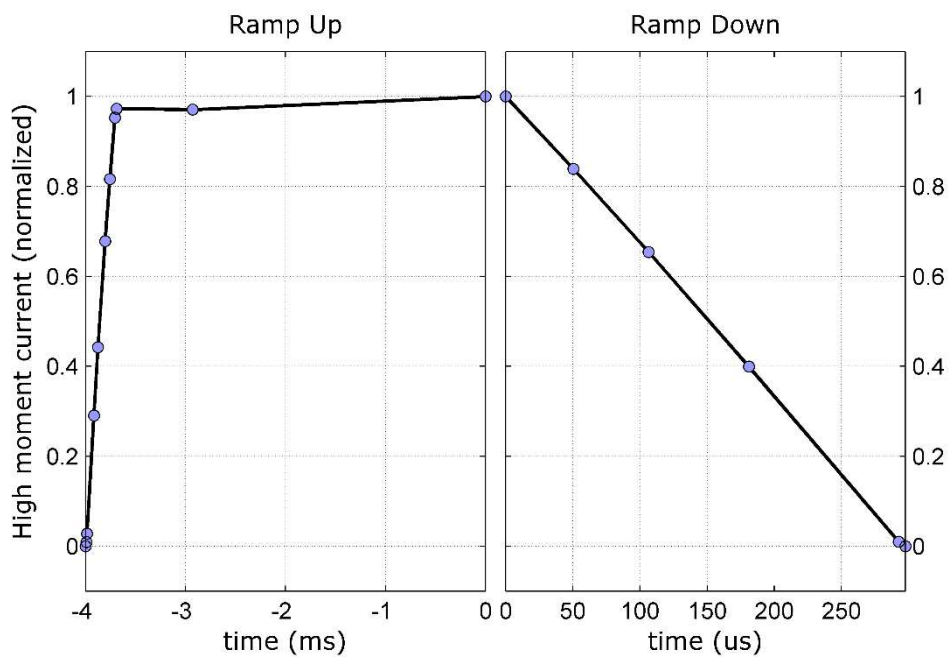


Figure 6. Ramp up and down for the HM waveform. The current is normalised.

Parameter	Value
Base frequency	210 Hz
Current range	5 Amp

Table 9: Waveform parameters for LM

Time [s]	Normalized current
-8.0000E-04	0.0000E+00
-7.4206E-04	9.8596E-02
-6.5865E-04	2.1171E-01
-2.8606E-04	6.4854E-01
0.0000E+00	1.0000E+00
7.3508E-07	9.9837E-01
1.2325E-06	9.4496E-01
1.7365E-06	8.6039E-01
2.5877E-06	7.3104E-01
3.2325E-06	6.0415E-01
4.6005E-06	3.8408E-01
5.4485E-06	2.7798E-01
6.5605E-06	1.6743E-01
7.8325E-06	9.1575E-02
9.3365E-06	3.9582E-02
1.0936E-05	1.5038E-02
1.3280E-05	0.0000E+00

Table 10: Normalized current waveform for LM

Parameter	Value
Base frequency	30 Hz
Current range	110 Amp

Table 11: Waveform parameters for HM

Time [s]	Normalized current
-4.0000E-03	0.0000E+00
-3.9899E-03	9.2172E-03
-3.9843E-03	2.7602E-02
-3.9159E-03	2.9080E-01
-3.8744E-03	4.4249E-01
-3.8034E-03	6.7823E-01
-3.7565E-03	8.1645E-01
-3.7049E-03	9.5273E-01
-3.6892E-03	9.7276E-01
-2.9285E-03	9.7073E-01
0.0000E+00	1.0000E+00
5.0432E-05	8.3915E-01
1.0634E-04	6.5419E-01
1.8099E-04	3.9940E-01
2.9265E-04	9.5770E-03
2.9747E-04	0.0000E+00

Table 12: Normalized current waveform for HM

# Digital Data

The complete dataset of the SkyTEM survey is delivered as a Geosoft database (GDB) and a Geosoft xyz file, which can be used as input for further processing and gridding and as input to inversion and interpretation software. The channels of the GDB and xyz are described in Table 13.

## Channel description, Survey Data

Parameter	Explanation	Unit
Fid	Unique Fiducial number	seconds
Line	Line number	LLLLLL
Flight	Name of flight	yyyymmdd.ff
DateTime	DateTime format	Decimal days
Date	Date	yyyymmdd
Time	Time	HH:MM:SS.ss
AngleX	Angle in flight direction	Degrees
AngleY	Angle perpendicular to flight direction	Degrees
Height	Filtered transmitter terrain clearance	Meters
Lon*	Latitude/Longitude, WGS84	Decimal degrees
Lat*	Latitude/Longitude, WGS84	Decimal degrees
E*	UTM zone 15N (WGS84)	Meter
N*	UTM zone 15N (WGS84)	Meter
DEM	Digital Elevation Model	Meters above sea level
Alt	DGPS Altitude	Meters above sea level
GdSpeed	Ground Speed	km/h
Curr_LM	Current, low moment	Amps
Curr_HM	Current, high moment	Amps
LM_Z_G01[xx]**	Geosoft array channels normalized LM dBdt Z-coil value. Voltage/(Tx moment*RX area)	pV/(m4*A)
HM_Z_G01[xx]**	Geosoft array channels normalized HM dBdt Z-coil value. Voltage/(Tx moment*RX area)	pV/(m4*A)
HM_X_G01[xx]**	Geosoft array channels normalized dBdt HM X-coil value. Voltage/(Tx moment*RX area)	pV/(m4*A)
PLNI_60Hz	Powerline Noise intensity (60Hz)	
Bmag_raw	Total Magnetic Intensity (1 Hz) Magnetic base station data	nT
Diurnal	Diurnal variation Magnetic base station data	nT
Mag_Raw	Total Magnetic Intensity Raw magnetic data	nT
Mag_Cor	Magnetic Intensity Filtered and diurnal corrected	nT
RMF	Residual magnetic Field Final corrected data	nT
TMI	Total Magnetic Intensity IGRF recalculated	nT

Table 13 Channel description, survey data

\*) Data positions refer to the center of the frame.

\*\*\*) The first valid gates are: Gate 9 (LM), Gate 16 (HMZ) and Gate 17 (HMX).

## Inversion results

The result of the spatially constrained inversion (SCI) is delivered as a Geosoft database (GDB) and Geosoft xyz containing the modelled layer conductivity. The channels of the GDB and xyz are described in Table 14.

The applied gridding methods, cell size, blanking distance and filtering are listed in Table 15.

### Channel description, EM inversion database

Parameter	Explanation	Unit
Line	Line number	LLLLLL
E	UTM Zone15N (WGS84)	Meter
N	UTM Zone15N (WGS84)	Meter
DTM	Digital Terrain Model	Meters above mean sea level
ResI1	Residual of data	-
Height	Filtered Height Measurement	Meter
InvHei	Inverted Height	Meter
DOI	Depth of Investigation	Meter
DOI_elevation	Depth of Investigation	Meters above sea level
Elev_array[xx]	Elevation of top of layer xx	Meter
Con_array [xx]	conductivity of layer xx	mS/m
Con_doi_array [xx]	Conductivity of layer xx Masked below DOI	mS/m
RUnc_array[xx]	Relative uncertainty of layer xx	-

Table 14 Channel description, inversion results

### Gridding method and parameters

Area	Gridding algorithm	Gridding filter	Cell size	Blanking distance
All blocks	Minimum curvature	-	25 m	100 m

Table 15: Geosoft gridding



# Data processing and presentation

This section covers processing of auxiliary data, magnetic data, processing and inversion of EM data and presentations.

All devices (DGPS, Laser altimeters, inclinometers) are moved to the centre of the frame and corrected for the tilt of the frame hence all data positions refer to the center of the frame. Data is split at the beginning and end of each planned flight line.

After the initial filtering, all data are resampled to 10Hz.

## Auxiliary data

### **Tilt processing**

The X and Y angle processing involves manual and automated routines using a combination of the SkyTEM in-house software SkyLab and Geosoft.

The processing involves the following steps:

1. 3 sec box filter (SkyLab)
2. Low pass filtering of 3.0 sec. (Geosoft)

### **Height processing**

The height processing involves manual and automated routines using a combination of the SkyTEM in-house software and Geosoft.

The processing involves the following steps:

1. Keeping the highest values pr. second and discarding the rest to correct for the canopy effect (treetop filter)
2. Tilt correction
3. Averaging of the two laser values.
4. Additional filters:
  - a. Low pass filter of 3.0 sec (Geosoft)

### **DGPS processing**

The DGPS has been processed using the Waypoint GrafNav Lite Differential GPS processing tool. The standard airborne settings have been used.

1. Import of base station (Master)
2. Import of airborne files (Rover)
3. Download of Precise Clocks and Ephemerides
4. Calculation of forward and reverse DGPS solution
5. Export as .txt file

The DGPS.txt files are used as input to the SkyLab software assuring DGPS corrected data in the processed files.

The ground speed, altitude, latitude and longitude from the processed DGPS' are imported into Geosoft and merged into the final database where the coordinates are converted into UTM Zone15N (WGS84) and a low pass filter of 3.0 sec is applied.

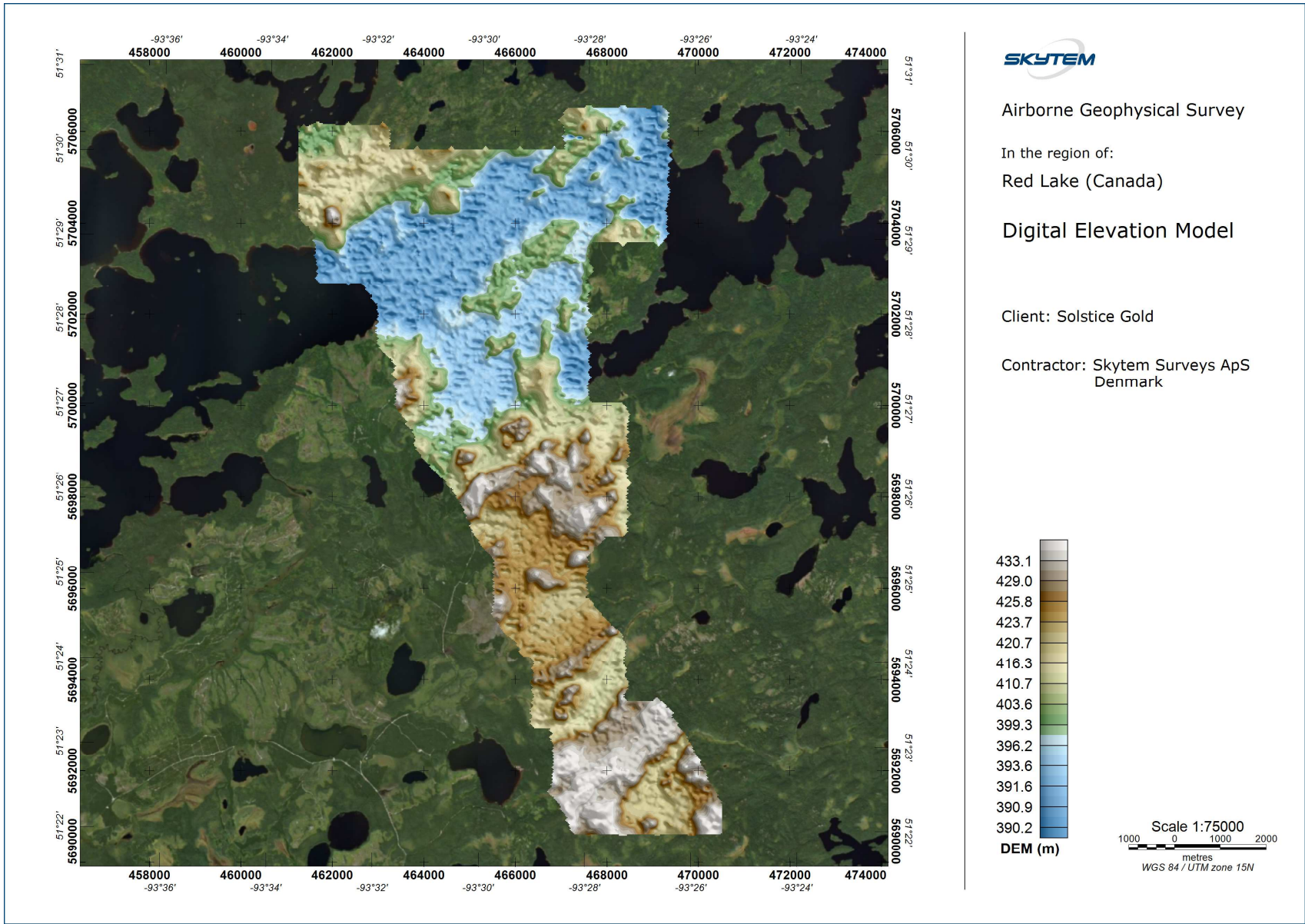
### **Digital elevation model**

A digital elevation model (DEM) has been calculated by subtracting the filtered laser altimeter data from the DGPS elevation. All steps related to the DEM are carried out Geosoft.

The processing of the final DEM involves the following steps:

1. Filtering and processing of the laser altimeter height as described above
2. DEM data received by subtraction of final filtered laser data from final processed DGPS altitude data

Figure 7 shows the DEM.



2022/01/13

Figure 7. DEM.

## Magnetic data

Final processing of the magnetic data involves the application of traditional corrections to compensate for diurnal variation effects. Geosoft magnetic data processing tools are applied as follows:

- Processing of static magnetic data acquired on magnetic base station
- Pre-processing of airborne magnetic data
  - Stacking of data to 10 Hz in SkyLab.
  - Moving positions to the center of the system in SkyLab.
- Processing and filtering of airborne magnetic data
- Standard corrections to compensate the diurnal variation
- IGRF correction
- Gridding

### **Processing of base station magnetic data**

The base station magnetometer data was merged into the base station Geosoft database daily for further processing.

The following filtering was applied:

- Fraser Low-pass filter (width 60 sec)
- The first day average (56881.6 nT) of the base data was subtracted to calculate the diurnal.

Processed diurnal magnetic data from the magnetic base station representing short term variations was merged with airborne magnetic data.

### **Processing and Filtering of airborne magnetic data**

Airborne magnetic data is filtered and interpolated as follows:

- Adjustment of the data for the time lag between the GPS position and the position of the magnetic sensor
- Data resampling to 10 Hz (stacking)
- Manual despiking to remove spikes and spurious data
- Geosoft processing:
  - Non-linear filter (3 sec)
  - Interpolation (Akima)
  - LP filter (3 sec)

### **Corrections to the magnetic data**

The following corrections are applied to the airborne magnetic data:

- Correction for diurnal variation using the digitally recorded ground base station magnetic values as described above
- Lag and heading were negligible and no correction was applied
- IGRF correction

### **IGRF correction**

The International Geomagnetic Reference Field (IGRF) is a long-wavelength regional magnetic field calculated from permanent observatory data collected around the world. The IGRF is updated and determined by an international committee of geophysicists every 5 years. Secular variations in the Earth's magnetic field are incorporated into the determination of the IGRF.

The IGRF model is calculated before levelling using the following parameters:

IGRF model year: 2020

Date: variable according to date channel in database

Position: variable according to GPS WGS84 longitude and latitude

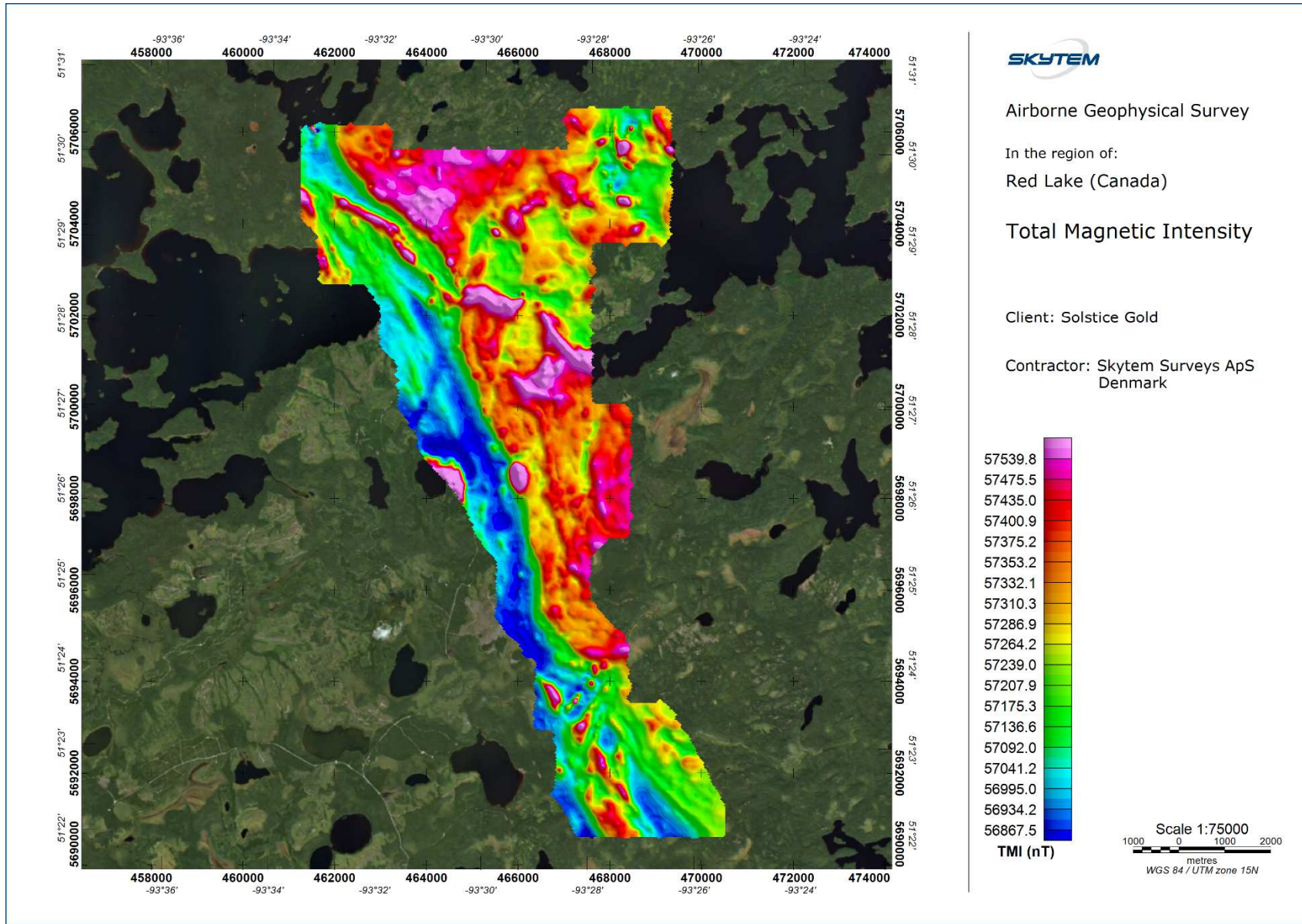
Elevation: variable according to magnetic sensor altitude derived from DGPS data

### **RMF and TMI recalculation**

The outcome of processed magnetic data after all corrections and levelling is the Residual Magnetic Field (RMF).

Total magnetic intensity (TMI) is recalculated to an altitude as flown at the survey area average altitude (460 m) by adding the IGRF regional field back to RMF on a fixed date (2021/11/10) for each individual point.

Figure 8 show the Total magnetic intensity map.



2022/01/12

Figure 8. Total Magnetic Intensity - TMI.  
SkyTEM Survey – Red Lake – January 2022



## EM data

This section covers processing of EM data, including primary field correction (PFC) and filtering of EM data.

### **Primary Field Compensation (PFC)**

The magnetic field coupling between the receiver coils and the transmitter loop is continuously hardware-monitored, providing a separate value for the magnetic field coupling during each transient sounding. These data are used for raw data correction in a separate post-processing step. The primary field compensation technique has proven stable and has routinely yielded a reduction of the primary field influence in very early time gates by a factor exceeding 50.

### **EM Filtering**

The PFC data is the input for further processing. The data are normalized in respect to effective Rx coil area, Tx coil area, number of turns and current giving the unit [pV/(m<sup>4</sup>\*A)].

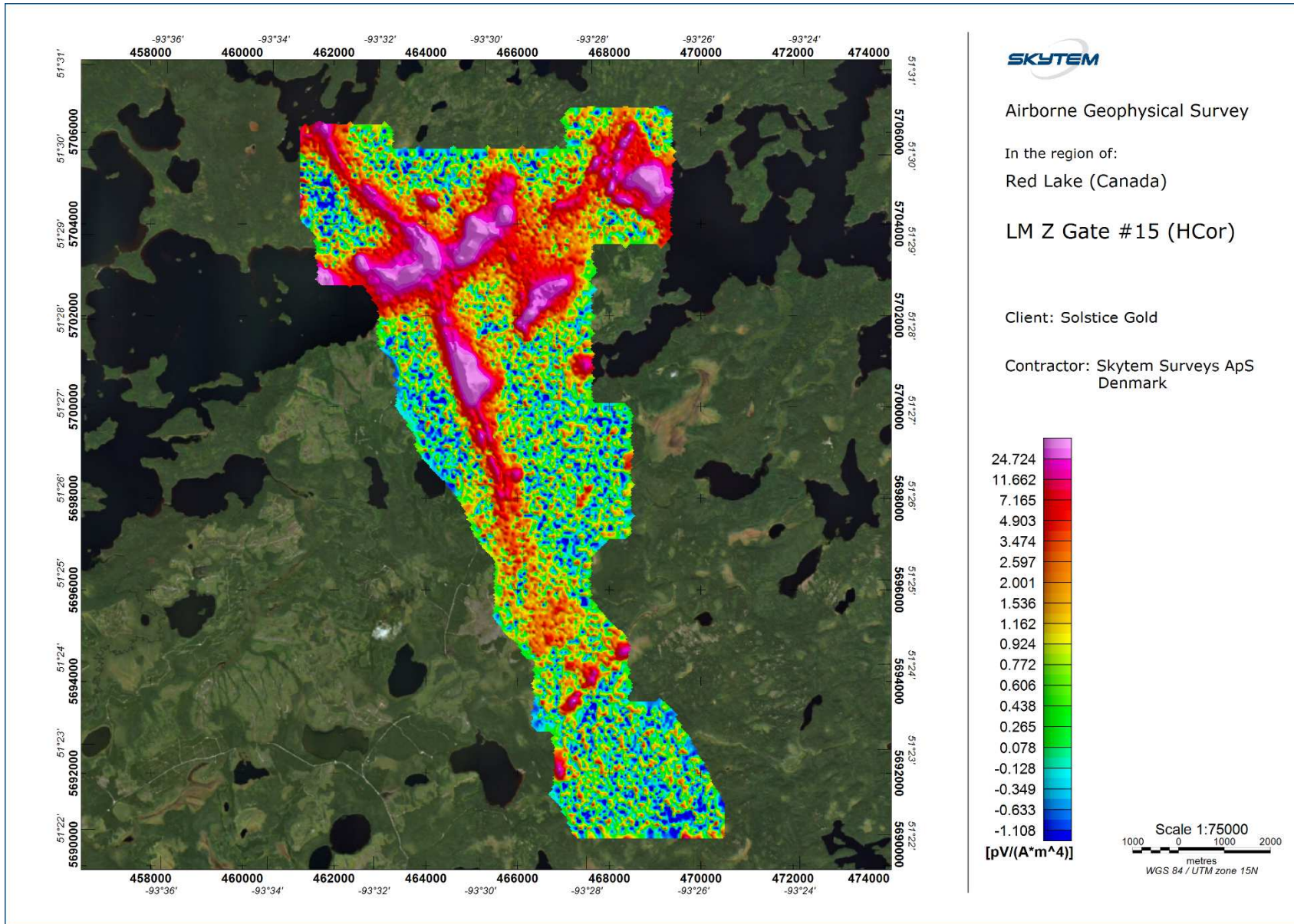
The EM data is filtered adaptively based on the signal-to-noise ratio. The applied EM filtering method is based on iterative weighted spline fitting routines, which operate in positive/negative symmetric transform spaces. The data weighting scheme relies on an extensive noise evaluation performed on the individual gate values of the raw data decays. Optimised sets of averaging filters are used for each measured moment and type of receiver coil in a stepwise averaging process. This allows for optimal suppression of motion induced noise as well as cultural noise components, while keeping track of the resulting data uncertainty.

The provided EM grids are corrected for variations in flying height. All grids are shifted to a level as if the survey were flown in a constant height of 50 m above the ground.

No height correction has been applied to the raw EM data channels in the delivered Geosoft database and data file.

Figure 9 and Figure 10 show examples of the LM Z and HM Z data. Geosoft grids of EM Z channels are included in the digital data delivery.

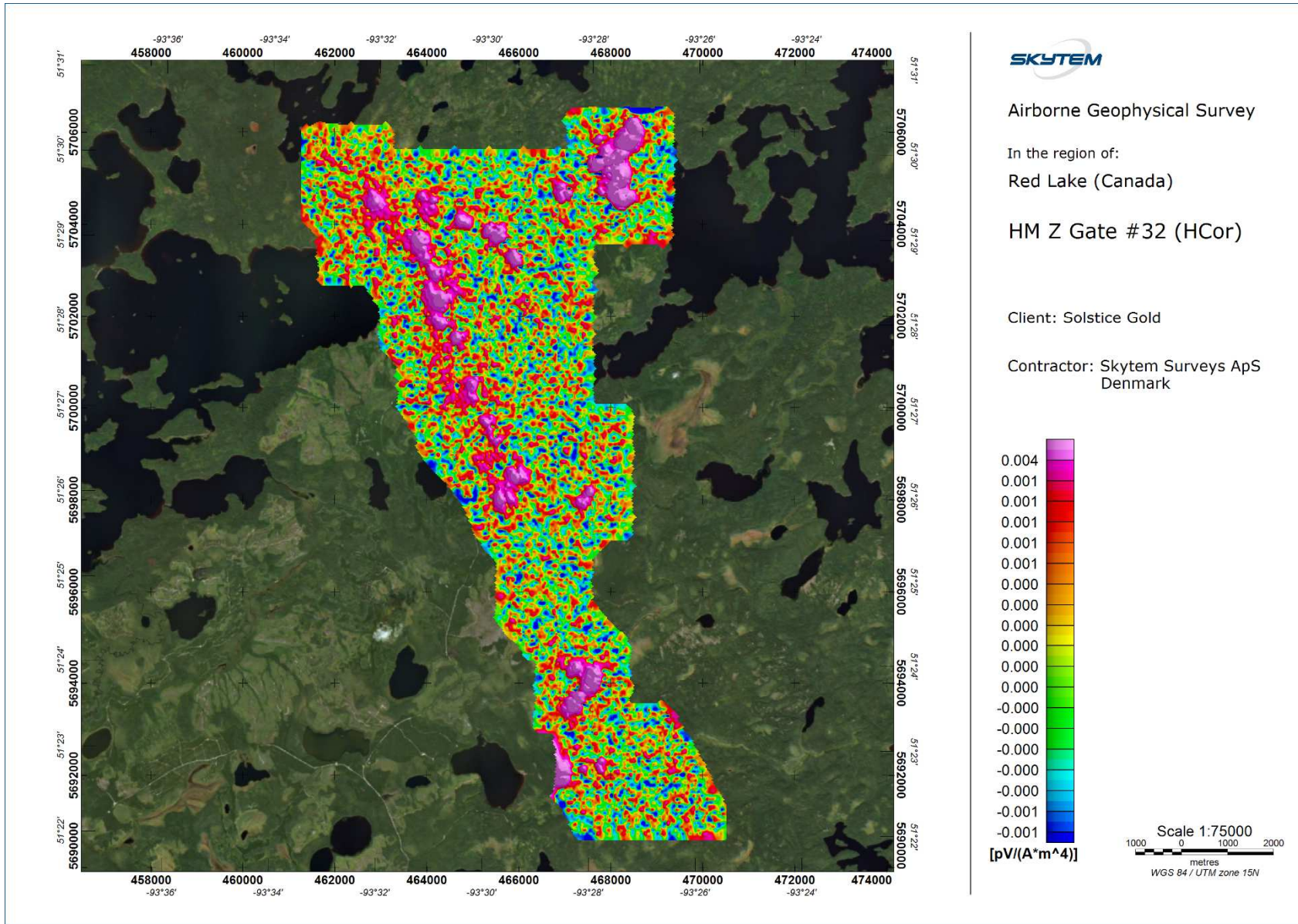




2022/01/12

Figure 9. Low Moment gate 15.

SkyTEM Survey – Red Lake – January 2022



2022/01/13

Figure 10. High Moment gate 25.

## Power Line Noise Intensity (PLNI)

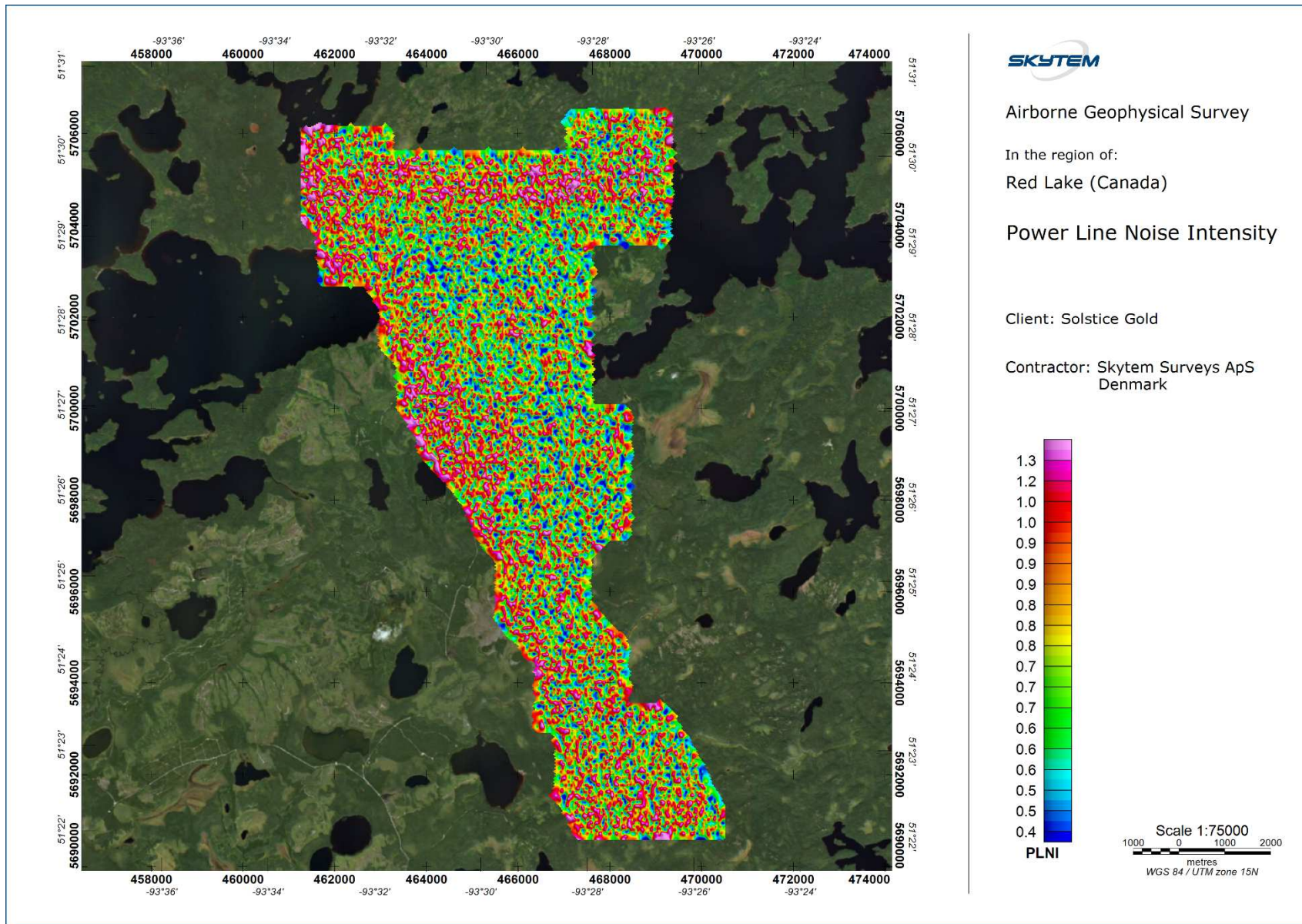
The PLNI is a powerful tool for identifying power line noise effect on EM and magnetic data. The PLNI monitor values are derived from a frequency analysis of the raw Z-component EM data. The Fourier transformation is evaluated at the local power transmission frequency yielding the amplitude spectral density of the power line noise.

CAUTION - When evaluating the PLNI values one should be aware of the following factors that may give rise to anomalous PLNI patterns unrelated to the actual power line noise level:

- Other noise sources than power line noise may contribute to the total noise spectral density in the data at the power transmission frequency. When power line noise is present it tends to dominate all such other noise sources.
- The presented PLNI values are not corrected for fly height or frame angles, which means that adjacent lines crossing the same power line may not exhibit the same values of PLNI.

Figure 11 shows the PLNI.





2022/01/12

Figure 11. Power line noise intensity

## Inversion

In this section, the particulars of modelling and inversion of SkyTEM data from Red Lake will be described.

The SkyTEM data have been processed and inverted using spatially constrained inversion (SCI) in Aarhus Workbench, a unique software package initially developed at Aarhus University, Denmark. In this SCI algorithm a group of time-domain EM (TEM) soundings are inverted simultaneously using 1-D models. Each sounding yields a separate layered model, but the models are constrained laterally. See Figure 12.

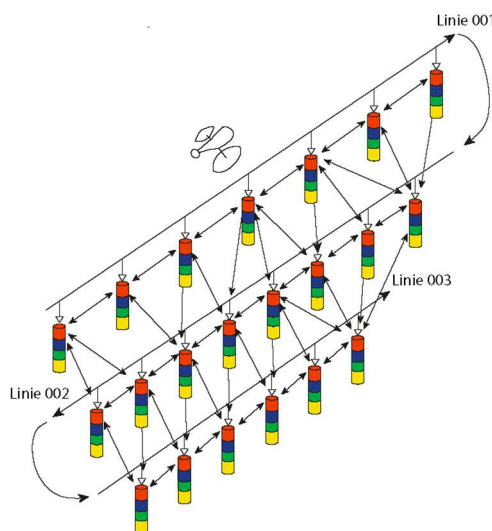


Figure 12. Schematic presentation of the SCI setup. Constraints connect not only soundings located along the flight line, but also those across them (figure from [hgg.au.dk](http://hgg.au.dk)).

### Initial model and optimisation norm

The SCI code is run in multi-layer, smooth-model mode in which the layer thicknesses are fixed, and the data are inverted only for conductivity.

In the inversion the thickness of the first layer is set to 4 m and the depth to the top of the deepest layer boundary is 500 m. While computing the layer thicknesses, the first and last layer boundary scales the model thicknesses automatically using a log distribution. Thicknesses and depths to the top of each layer for the current project are given in the table below.

The input data to the inversion are the LM and HM dB/dt Z-component EM data. The initial model conductivity structure is a homogenous half-space model with an Auto Calculated starting conductivity.

Manually masking of data displaying coupling effects e.g. due to power lines is not part of the current project and therefore cultural effects in the EM data can be present in the final data base.

Note: Prior to the inversion EM data with relative uncertainties higher than 0.40 have been masked.

Layer #	Layer Thickness [m]	Depth to top of layer [m]
1	4.0	0
2	4.4	4.0
3	4.8	8.4
4	5.2	13.1
5	5.7	18.3
6	6.2	24.0
7	6.7	30.1
8	7.3	36.8
9	8.0	44.2
10	8.7	52.2
11	9.5	60.9
12	10.4	70.4
13	11.3	80.8
14	12.3	92.0
15	13.4	104.4
16	14.6	117.8
17	16.0	132.4
18	17.4	148.4
19	19.0	165.8
20	20.7	184.8
21	22.6	205.5
22	24.6	228.1
23	26.8	252.7
24	29.3	279.6
25	31.9	308.8
26	34.8	340.8
27	37.9	375.6
28	41.4	413.5
29	45.1	454.9
30	-	500.0

*Table 16 Layer distribution of the multi-layer smooth inversion model.*

## **Model Presentation - Model sections and maps**

The models resulting from the inversion are presented as layer conductivity profiles and as grids and maps of mean conductivity in depth intervals in Geosoft and pdf format. Figure 13 and Figure 14 show examples of a layer conductivity profile and map respectively. All profiles, grids, images and maps are included in the digital data delivery.

### **Model Sections**

The profile plots consist of four sections; the top section shows the inverted models, with topography, where the conductivity of the individual layers is colour coded according to the colour bar. The conductivity is shown on a logarithmic scale and conductive and resistive features appear with the same weight. The thin grey line indicates the upper DOI. The white shading in the analysis section indicates the estimated depth of investigation (DOI). Where the colour fades into the white, the inverted conductivity is determined almost exclusively by the regularization, i.e. the conductivity is essentially undetermined. The measured and inverted flight elevation is shown with a black and blue line, respectively, above the model section.

The second and the third section show the measured data (dots) together with the response of the inverted models (solid lines) for low moment data (LMZ) and high moment data (HMZ). Blank sections in the profile indicate areas where the signal to noise ratio has been too low for any data to be used in the inversion. Essentially the resistivity in those sections can be considered as "Very high" ( $>1000 \Omega\text{m}$ ). Alternatively, data have been negative, or a man-made conductor has interfered with the signal, which can also lead to data being discarded prior the inversion.

The bottom section shows the data residual (black dots) of the inversions.

In the section to the right, an overview map of the survey with an indication of the given line and flight direction is seen.

The quality of the inversion results can be evaluated by inspecting the residuals. The data residual is calculated by comparing the measured data with the response of the resulting model after inversion. If the residual is in the range of 1, the misfit between the response of the final model and the data is, on average, equal to the noise. If the residual is high, it might be caused by data that are noisier than the noise model takes into account. This can be seen where resistivity is very high and the signal consequently very low. A high data residual can also be due to the inconsistency between the 1D model assumed in the inversion and the 2D/3D character of the real world. These are found primarily at the edges of sharp lateral conductivity contrasts. Finally, coupling effects due to power lines and other manmade conductors can also be a source of a high residual as well as the presence of induced polarization in the EM data.



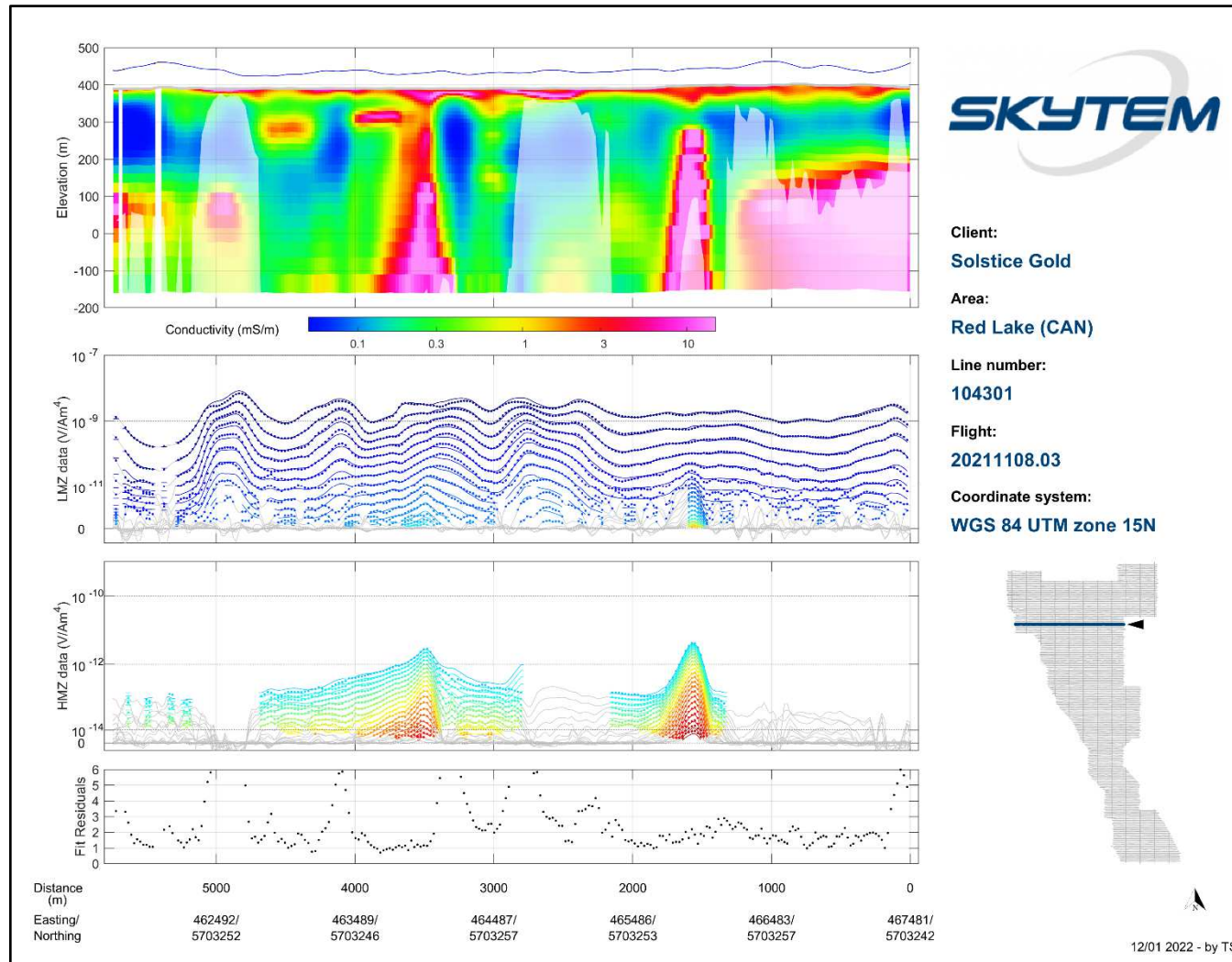


Figure 13 Example of section plot. From top to bottom: conductivity section with flight height and Depth of Investigation (DOI), LM and HM gate plot (data=dots, model=line), residual.

**Layer conductivity maps**

The layer conductivity maps show the inverted conductivity for each of the model layers. As the thickness of the model layers increases downwards the maps represent a varying thickness interval. The depth intervals for each layer are stated on the maps in meters below the surface.

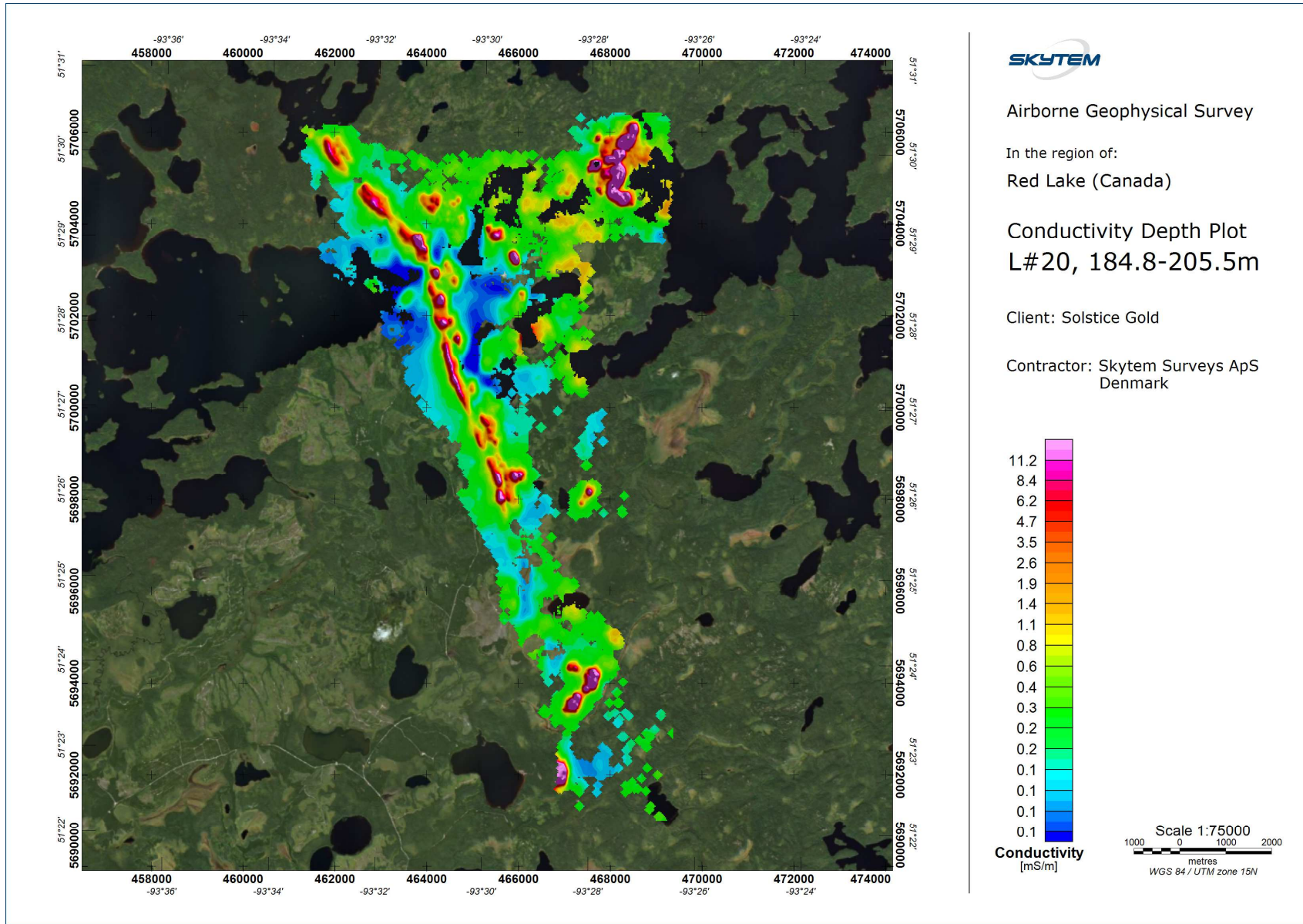


Figure 14 Modelled Layer Conductivity of layer 20 (depth 184.8 m – 205.5 m).

## References

Aarhus University, n.d., Guide to 1D-LCI inversion.

Auken, E., Foged, N. and Sørensen, K., 2002, Model recognition by 1-D laterally constrained inversion of resistivity data: Proceedings – New Technologies and Research Trends Session, 8<sup>th</sup> meeting, EEGS-ES.

Auken, E., Christiansen, A. V., Jacobsen, B. H., Foged, N., and Sørensen, K. I., 2005, Piecewise 1D Laterally Constrained Inversion of resistivity data: *Geophysical Prospecting*, 53, 497–506.

Christiansen, A.V. and Auken, E., 2012, A global measure for depth of investigation: *Geophysics*, vol 77, No. 4, 171-177.

Sattel, D., 2005, Inverting airborne electromagnetic (AEM) data with Zohdy's method, *Geophysics*, 70, G77-G85.

## Appendix list

Appendix 1: Instruments

Appendix 2: Introduction to Spatially Constrained Inversion (SCI)

# Appendix 1: Instruments

# Instrument positions

The instrumentation involves a time domain electromagnetic system, two inclinometers, two altimeters and two DGPS'.

The measurements were carried out, using a setup as described below.

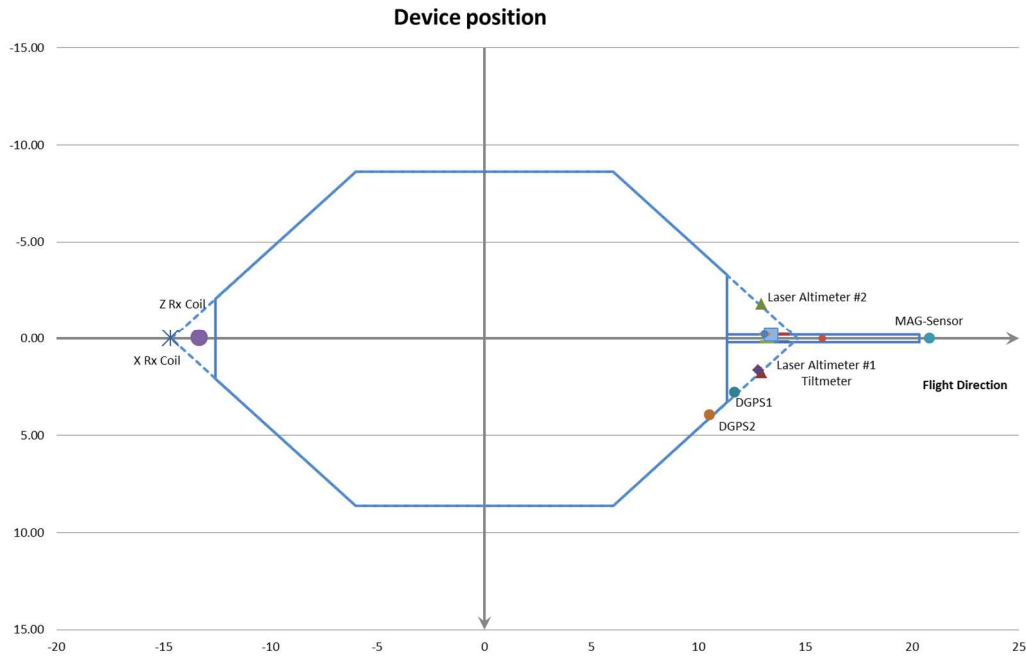


Figure 1 Sketch showing the frame and the position of the basic instruments. The blue line defines the transmitter loop. The horizontal plane is defined by  $(x, y)$ .

The location of instruments in respect to the frame is shown in Figure 1 and is given in  $(x, y, z)$  coordinates in the table below.

X and y define the horizontal plane. Z is perpendicular to  $(x, y)$ . X is positive in the flight direction, y is positive to the right of the flight direction, and z is positive downwards.

The generator used for powering of the transmitter is  $\sim 30$  m m below the helicopter.



Device	X	Y	Z
DGPS1 (EM)	11.68	2.79	-0.16
DGPS2 (EM)	10.51	3.95	-0.16
HE1 (altim.)	12.94	1.79	-0.12
HE2 (altim.)	12.94	-1.79	-0.12
Inclinometer 1	12.79	1.64	-0.12
Inclinometer 2	12.79	1.64	-0.12
RX (Z Coil)	-13.35	0.00	-2.00
RX (X Coil)	-14.65	0.00	0.00
Mag sensor	20.50	0.00	-0.56

For the location of instruments see Figure 1.

## Transmitter

The time domain transmitter loop can be described as an octagon with the corners listed below:

X	Y
-12.64	-2.10
-6.14	-8.58
6.14	-8.58
11.41	-3.31
11.41	3.31
6.14	8.58
-6.14	8.58
-12.64	2.10

The total area of the transmitter coil defined by the corner points is 342 m<sup>2</sup> and 68.3 m in circumference.

The key parameters defining the transmitter set up are:

#### Low Moment

Parameter	Value
Number of transmitter turns	2
Transmitter area	342 m <sup>2</sup>
Peak current	5 Amp
Peak moment	~3,000 NIA
Repetition frequency	210 Hz
On-time	800 μs
Off-time	1581 μs
Duty cycle	33 %
Wave form	Triangular

#### High Moment

Parameter	Value
Number of transmitter turns	12
Transmitter area	342 m <sup>2</sup>
Peak current	110 Amp
Peak moment	~500,000 NIA
Repetition frequency	30 Hz
On-time	4000 μs
Off-time	12667 μs
Duty cycle	24%
Wave form	Square



*Figure 2 The 342 m<sup>2</sup> frame in production mode.*

## Receiver system

The decay of the secondary magnetic field is measured using two independent active induction coils. The Z coil is the vertical component, and the X coil is the horizontal in-line component. Each coil has an effective receiver area of 325 m<sup>2</sup> (Z), 115 m<sup>2</sup> (X).

The receiver coils are placed in a null-position:

Z coil (x, y, z) = (-13.32 m, 0.0 m, -2.0 m)

X coil (x, y, z) = (-14.65 m, 0.0 m, 0.0 m)

In the null-position, the primary field is damped with a factor of 0.01 on HM and due to PFC correction, it can be neglected on LM.



Figure 3 Rudder containing the Z coil located in the top part of the tower.

The key parameters defining the receiver set up are:

Receiver parameters		
Sample rate		All decays are measured
Number of output gates		37 (HM) and 28 (LM)
Receiver coil low pass filter		204 kHz (Z-coil) and 343 kHz (X-coil)
Receiver instrument low pass filter		300 kHz
Repetition frequency	LM	210 Hz
	HM	30 Hz
Front gate	LM	0 $\mu$ s
	HM	370 $\mu$ s

Receiver gate times are measured from the start of the transmitter current turn-off. A complete list describing gate open, close, and centre times are listed in the main report.

# Inclination

Instrument type: Bjerre Technology

The inclination of the frame is measured with 2 independent inclinometers. The x and y angles are measured 2 times per second in both directions. The inclinometers are placed in the rear of the frame as close to the z coil as possible, see Figure 1.

The angle data are stored as x, y readings. X is parallel to the flight direction and positive when the front of the frame is above horizontal. Y is perpendicular to the flight direction and negative when the right side of the frame is above horizontal.

The angle is checked and calibrated manually within 1.0 degree by use of a level meter.

# DGPS airborne unit and base stations

Chipset: OEMV1-L1 14-channel rate.

Antenna: Trimble, Bullet III GPS Antenna

The differential GPS receiver is on top of the boom in front of the frame.

The DGPS delivers one dataset per second. The raw coordinates are given in Latitude/Longitude, WGS84.

The uncertainty in the xyz-directions is  $\pm 1$  m after processing.

The processed DGPS data is combined with the EM data in the xyz-files, giving the precise position.

DGPS parameters	
Sample rate	1 HZ
Uncertainty	$\pm 1$ m

# Altimeter

Instrument type: MDL ILM300R

Two independent laser units mounted on the frame measuring the distance from the frame to the ground, see Figure 1

Each laser delivers 30 measurements per second, and covers the interval from 0.2 m to approximately 200 m.

Dark surfaces including water surfaces will reduce the reflected signal. Consequently, it may occur that some measurements do not result in useful values.

The altimeter measurements are given in meters with two decimals. The uncertainty is 10 - 30 cm. The lasers are checked on a regular basis against well-defined targets.

Laser parameters	
Sample rate	30 Hz
Uncertainty	10 - 30 cm
Min/ max range	0.2 m / 200 m

# Magnetometer airborne unit

Instrument type: Geometrics G822A sensor and Kroum KMAG4 counter.

The Geometrics G822A sensor and Kroum KMAG4 counter is a high sensitivity Cesium magnetometer. The basic of the sensor is a self-oscillating split-beam Cesium vapor (non-radioactive) Principe, which operates on principles similar to other alkali vapor magnetometers.

The sensitivity of the Geometrics G822A sensor and Kroum KMAG4 counter is stated as  $<0.0005 \text{ nT}/\sqrt{\text{Hz}}$  rms. Typically 0.002 nT P-P at a 0.1 second sample rate, combined with absolute accuracy of 3 nT over its full operating range.

The magnetometer is synchronized with the TEM system. When the TEM signal is on, the counter is closed. In the TEM off-time the magnetometer data is measured from 100 microseconds until the next TEM pulse is transmitted. The data are averaged and sampled as 60 Hz.

Parameter	Value
Sample frequency	60 Hz (in between each HM EM pulse)

# Magnetometer base station

Instrument type: GEM Proton.

The GEM Proton is a portable high-sensitivity precession magnetometer.

The GEM Proton is a secondary standard for measurement of the Earth's magnetic field with 0.01 nT resolutions, and 1 nT absolute accuracy over its full temperature range.

The base station data are sampled with 1 Hz frequency.



## Appendix 2: Introduction to Spatially Constrained Inversion (SCI)

## Model and inversion routine

The SkyTEM data have been processed and inverted using a spatially constrained inversion (SCI) in Aarhus Workbench, a unique software package initially developed at Aarhus University, Denmark. In the SCI algorithm, a group of time-domain EM (TEM) soundings are inverted simultaneously using 1-D models (Auken et al. 2002 & 2005, Viezzoli et al. 2008). Each sounding yields a separate layered model, but the models are constrained spatially on resistivity, see Figure 1 .

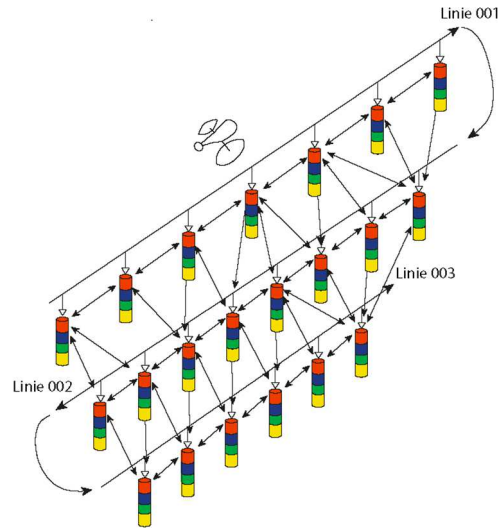


*Figure 1 Schematic presentation of the SCI setup. Constraints connect not only soundings located along the flight line, but also those across them (figure from hgg.au.dk).*

The result of the SCI inversion is a quasi-3D model that varies smoothly along and across the profiles. The SCI inversion is capable of simultaneously inverting the interleaved HM and LM measurements, yielding a conductivity model that combines the very good shallow depth resolution offered by the low moment data and the larger depth of investigation from the high moment data.

The SCI code is run in multi-layer, smooth-model mode, in which the layer thicknesses are fixed and the data are inverted only for resistivity. The SCI smooth-model inversion typically uses 20-30 layers. Smoothness constraints are applied on the variation of resistivity with depth, in addition to the lateral constraints between adjacent models. Multi-layer smooth-model inversion is slower to compute, but is usually able to provide a very close fit to the observed data.

In the model set-up the thickness of the first layer and the depth to the top of the deepest layer boundary is given. While computing the layer thicknesses, the first and last layer boundary scales the model thicknesses automatically using a log distribution.

The input data to the inversion are the LM & HM moments of the Z-component of EM data. Both moments are combined in a single inversion to increase the depth resolution. The initial model resistivity structure is a homogenous half-space model with an Auto Calculated starting resistivity.

Constraints are given as factors, i.e. a factor of 1.1 means that the parameter can vary between the starting value divided by/times 1.1 (Aarhus University).

The SCI inversion allows for horizontal and vertical constraints to be set for resistivities.

Horizontal constraints are scaled by distance using a reference distance and power function:

$$C = 1 + (C_{opt} - 1) \left( \frac{\Delta GPS}{Dist_{ref}} \right)^n$$

Where  $C$  is the used constraint,  $C_{opt}$  is the optimal constraint at a sounding distance of  $Dist_{ref}$  and  $\Delta GPS$  is the actual sounding distance.

The horizontal constraints are initially scaled by distance and a power function.

Inversion for flight altitude is included after the first 5 inversion runs. The constraint on the processed flight height is set low and is only allowed a very limited variation.

The methodology for calculating the DOI is based on a recalculated Jacobian matrix from a 1D model (Christiansen and Auken, 2012). Working with global and absolute threshold values requires a relative, data-type, independent relation between the model space and data space, which we obtain by working in the logarithmic model and data spaces. For a given model, the DOI calculations solely include information from the part of the Jacobian relating to the observed data. This means that lateral or vertical model constraints or a priori information, which also contributes information to the model, is not included. The workflow includes the following steps:

- 1) Starting from a measured data set, the data is inverted into a smooth model. The inversion includes the data uncertainty, estimated from the data stack, and the regularization method of the chosen inversion algorithm.
- 2) The Jacobian for the sub-discretized model is calculated.
- 3) The Jacobian is finally used to compute the cumulated sensitivities from which we can deduct the DOI.

### **Data and noise model**

The inaccuracy of TEM data is influenced by the ambient noise. This noise is reduced by selective stacking of delay time series and by applying appropriate filters in the receiver system.

### **Data insufficiency**

For SkyTEM data, the insufficiency lies primarily in the limited delay time range that can be obtained. The earliest obtainable time gate is determined by the

turnoff of the Tx current, and the latest useful time gate is determined by the signal to noise ratio. Increasing the Tx moment will give better measurements at late times, and thus improve the depth penetration, but also increase the turnoff time and thus remove early-time gates, thereby making the near-surface resolution poorer. This trade-off is solved by transmitting an alternating sequence of (1) a low moment that can be turned off quickly to give good near-surface resolution, and (2) a high moment that will improve the signal-to-noise ratio at late times, thus improving depth penetration.

### **Model inconsistency**

When using 1D models in the interpretation of SkyTEM data, inconsistency arises where the lateral gradient of conductivity is not small, e.g. typically in mining applications. However, also in environmental investigations, inconsistencies can arise, typically where near-surface good conductors have abrupt boundaries. Often such inconsistency is indicated by the data residual being high and one should look upon the inversion results with some caution at these locations. 3D effects can also reveal themselves by the so-called 'pant legs', i.e. conductive or resistive structures projecting at an angle of approximately 30 degrees from the horizontal at the edges of high contrast structures.

Work Type	Vendor	unit	total unit work	\$ expenditure /per unit(line Km)	Total Invoice	Work date from	Work date to
High-res MAG survey	SkyTEM Canada Inc	line km	879	\$339.48	298,402.00	05-Nov-21	15-Nov-21
Reporting	Geologist-Sandy Barham	days	5	\$500/days	\$2,625.00	16-May-22	30-May-22
					<b>301,027.00</b>		